

THERMAL BUCKLING OF STRAIGHT TRACKS FUNDAMENTALS, ANALYSIS AND PREVENTIVE MEASURES



SEPTEMBER 1978
INTERIM REPORT

Document is available to the public through the
National Technical Information Service,
Springfield, Virginia 22161.

Prepared for
U.S. DEPARTMENT OF TRANSPORTATION
FEDERAL RAILROAD ADMINISTRATION
Office of Research and Development
Washington, D.C. 20590

NOTICE

This document is disseminated under the sponsorship of the Department of Transportation in the interest of information exchange. The United States Government assumes no liability for its contents or use thereof.

NOTICE

The United States Government does not endorse products or manufacturers. Trade or manufacturers' names appear herein solely because they are considered essential to the object of this report.

1. Report No. FRA/ORD-78/49		2. Government Accession No.		3. Recipient's Catalog No.	
4. Title and Subtitle THERMAL BUCKLING OF STRAIGHT TRACKS; FUNDAMENTALS, ANALYSES, AND PREVENTIVE MEASURES				5. Report Date September, 1978	
				6. Performing Organization Code TSC-744	
7. Author(s) Arnold D. Kerr				8. Performing Organization Report No. Princeton University 77-TR-6 DOT-TSC-FRA-78-14	
9. Performing Organization Name and Address Princeton University Department of Civil Engineering Princeton, NJ 08540				10. Work Unit No.	
				11. Contract or Grant No. DOT-TSC-1149	
12. Sponsoring Agency Name and Address U.S. Department of Transportation Federal Railroad Administration Office of Research and Development Washington, DC 20590				13. Type of Report and Period Covered Interim Report	
				14. Sponsoring Agency Code RRD-32	
15. Supplementary Notes U.S. Department of Transportation Under contract to: Transportation Systems Center Kendall Square Cambridge, MA 02142					
16. Abstract This report, written mainly for the practicing railroad engineer, explains the phenomenon of thermal buckling of straight tracks, shows how to analyze it, and describes measures for preventing it. Following an introductory discussion of track buckling problems caused by a temperature increase in the rails, the report describes the distribution of axial forces in the track rails caused by temperature changes. It reviews briefly track buckling test results obtained by a number of railroads. The method of analysis for the determination of a "safe temperature increase", recently developed by the author, is then discussed. To simplify the use of this analysis, the results are presented graphically for a wide range of track parameters, and the use of the presented graphs is demonstrated with examples. It is shown how the graphs may also be used for the determination of the rail installation temperature. The paper concludes with a description of track tests for obtaining the needed parameters, and a discussion of measures adopted by various railroads to prevent thermal track buckling.					
17. Key Words Railroad Track, Buckling of Tracks, Thermal Forces in Track, Track Maintenance,			18. Distribution Statement: Document Available from: National Technical Information Service Springfield, Virginia 22151		
19. Security Classif. (of this report) Unclassified		20. Security Classif. (of this page) Unclassified		21. No. of Pages 58	22. Price

PREFACE

This report was prepared as part of a research program sponsored by the Federal Railroad Administration, Office of Research and Development, contract DOT-TSC-1149. The program is being managed by the Department of Transportation, Transportation Systems Center, Dr. Andrew Kish, technical monitor. The research effort is aimed at creating a basis for the rational design, construction, and maintenance of railroad tracks.

The present report is written mainly for the practicing railroad engineer. It explains the phenomenon of thermal buckling of straight tracks, shows how to analyse it, and describes measures for preventing it. The report is the outcome of a study which was initiated by A. D. Kerr in the critical survey "Lateral Buckling of Railroad Tracks due to Constrained Thermal Expansions" (Princeton University/FRA Report 75-SM-8, Sept. 1975), and which led to the development of a new analysis presented in "An Analysis of Thermal Track Buckling in the Lateral Plane" (Report No. FRA-OR&D-76-285 Sept. 1976).

The author wishes to thank Stuart B. Bassler and W. Alex Dallis, Jr., students and undergraduate research assistants at Princeton University, for performing the numerical evaluations presented in this report.

METRIC CONVERSION FACTORS

Approximate Conversions to Metric Measures

Symbol	When You Know	Multiply by	To Find	Symbol
LENGTH				
in	inches	2.5	centimeters	cm
ft	feet	30	centimeters	cm
yd	yards	0.9	meters	m
mi	miles	1.6	kilometers	km
AREA				
in ²	square inches	6.5	square centimeters	cm ²
ft ²	square feet	0.09	square meters	m ²
yd ²	square yards	0.8	square meters	m ²
mi ²	square miles	2.6	square kilometers	km ²
	acres	0.4	hectares	ha
MASS (weight)				
oz	ounces	28	grams	g
lb	pounds	0.45	kilograms	kg
	short tons (2000 lb)	0.9	tonnes	t
VOLUME				
teaspoon	teaspoons	5	milliliters	ml
tablespoon	tablespoons	15	milliliters	ml
fluid ounce	fluid ounces	30	milliliters	ml
c	cup	0.24	liters	l
p	pint	0.47	liters	l
qt	quart	0.95	liters	l
gal	gallon	3.8	liters	l
ft ³	cubic feet	0.03	cubic meters	m ³
yd ³	cubic yards	0.76	cubic meters	m ³
TEMPERATURE (exact)				
F	Fahrenheit temperature	5/9 (after subtracting 32)	Celsius temperature	°C

Approximate Conversions from Metric Measures

Symbol	When You Know	Multiply by	To Find	Symbol
LENGTH				
mm	millimeters	0.04	inches	in
cm	centimeters	0.4	inches	in
m	meters	3.3	feet	ft
m	meters	1.1	yards	yd
km	kilometers	0.6	miles	mi
AREA				
cm ²	square centimeters	0.16	square inches	in ²
m ²	square meters	1.2	square yards	yd ²
km ²	square kilometers	0.4	square miles	mi ²
ha	hectares (10,000 m ²)	2.5	acres	ac
MASS (weight)				
g	grams	0.035	ounces	oz
kg	kilograms	2.2	pounds	lb
t	tonnes (1000 kg)	1.1	short tons	st
VOLUME				
ml	milliliters	0.03	fluid ounces	fl oz
l	liters	2.1	pints	pt
l	liters	1.06	quarts	qt
l	liters	0.26	gallons	gal
m ³	cubic meters	35	cubic feet	ft ³
m ³	cubic meters	1.3	cubic yards	yd ³
TEMPERATURE (exact)				
°C	Celsius temperature	9/5 (then add 32)	Fahrenheit temperature	°F

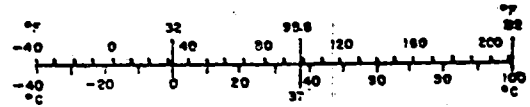
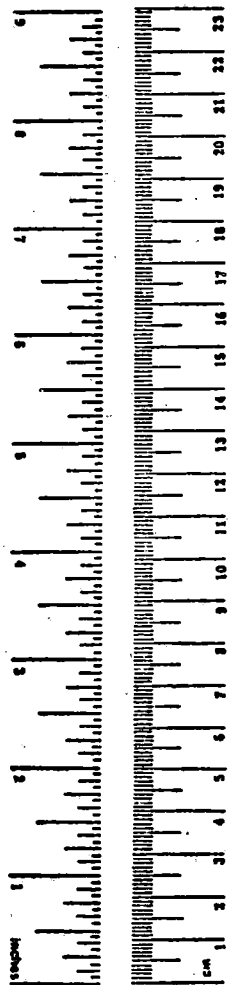


TABLE OF CONTENTS

<u>Section</u>	<u>Page</u>
1. INTRODUCTION	1
2. THE DISTRIBUTION OF RAIL COMPRESSION FORCES CAUSED BY A UNIFORM TEMPERATURE INCREASE	5
3. RESULTS OF THERMAL TRACK BUCKLING TESTS	10
4. ANALYSIS OF THERMAL TRACK BUCKLING	19
5. THE TRACK PARAMETERS NEEDED FOR THE PRESENTED ANALYSIS . .	33
6. EXAMPLES	36
7. MEASURES FOR PREVENTING THERMAL BUCKLING OF TANGENT TRACKS .	42
REFERENCES	45
APPENDIXES A. RAIL PROPERTIES.	49
B. REPORT OF INVENTIONS	50

LIST OF ILLUSTRATIONS

<u>Figure</u>		<u>Page</u>
1.	Buckled Railroad Tracks	3
2.	Axial Force Distribution in the Rails of a Straight Jointless Track	6
3.	Rail Temperature Increase vs. Axial Force in Rails	6
4.	Axial Force Distribution in a Track of Length L (based on the simplifying assumption $r_0 = \text{const}$)	8
5.	Free Body Diagram for the Determination of the Axial Force in the "Breathing" Region	8
6.	Buckling Modes Observed in Tests	11
7.	The Track Buckling Facility at Karlsruhe	12
8.	Rail-Tie Fasteners Used in Test Tracks	12
9.	Temperature Increase vs. Lateral Displacement Observed in Track Buckling Tests	16
10.	Distribution of Axial Compression Forces Before and After Buckling	20
11.	Resistances Between Rail-Tie Structure and Ballast	22
12.	Typical Equilibrium Branches for a Heated Straight Track	23
13.	Typical Equilibrium Branches for a Track with Lateral Geometric Imperfections	23
14.	Buckled Track Shapes Obtained from Analysis for $T_0 = 50^\circ\text{C}$ (90°F)	26
15.	Equilibrium Branches and Corresponding Axial Force Curves Obtained from Analysis	27
16.	Equilibrium Branches for 132 lb Track for Various Values of Rail-Tie Ballast Resistance	30
17.	Equilibrium Branches for 132 lb Track for Various Values of Rail-Tie Ballast Resistance	31
18.	Dependence of Safe Temperature Increase T_L on Track Parameters	32

LIST OF ILLUSTRATIONS (Cont'd)

<u>Figure</u>		<u>Page</u>
19.	Dependence of Lateral Resistance on Track Structure. Non-Compacted Ballast	35
20.	Dependence of Lateral Resistance on the Tonnage Carried Over Track	35
21.	Method for Establishing the Installation (Neutral) Temperature for a Railroad Track	39
22.	Determination of Rail Installation Temperatures for Extreme Temperature Conditions	41
23.	Measures for Increasing Lateral Resistance	44

LIST OF TABLES

<u>Table</u>		<u>Page</u>
1.	Test Results for P50 Track Sections with Wooden Ties and Cut-Spike Fasteners	17
2.	Dependence of v_{\max} and \tilde{N}_t on T_0 , for the 132 lb Track	28

1. INTRODUCTION

A railroad track consists of two parallel metal rails attached to closely spaced cross-ties which are embedded in a crushed-stone layer called the ballast. In a conventional track the rail ends are joined by bars and bolts which form an expandable joint.

Expandable rail joints weaken the track structurally, they increase the maintenance cost of tracks and rolling stock, and they increase the power consumption of a running train. Therefore, it is only natural that since the early days of railroad track construction there was a desire to eliminate many of the joints by increasing the length of the rails; with elimination of all joints (i.e. with the use of continuously welded rails) as a final goal.

A successful technique to weld rails (the Thermit method) was introduced at the turn of the century. The main reason why continuously welded rails were not installed at this early stage was the belief that, due to the elimination of the expansion joints, high axial compression forces would build up during the hot summer days and buckle the track.

The possibility of buckling of jointless tracks due to constrained thermal expansions was discussed, as early as 1902, by A. Haarmann [1].¹⁾ However, except for a few analytical attempts, this problem did not get the full attention of railroad research engineers until about thirty years later. Based on the experience gained since then with longer rails, and supported by findings of track buckling tests and results of related track analyses, thousands of miles of continuously welded rails were installed

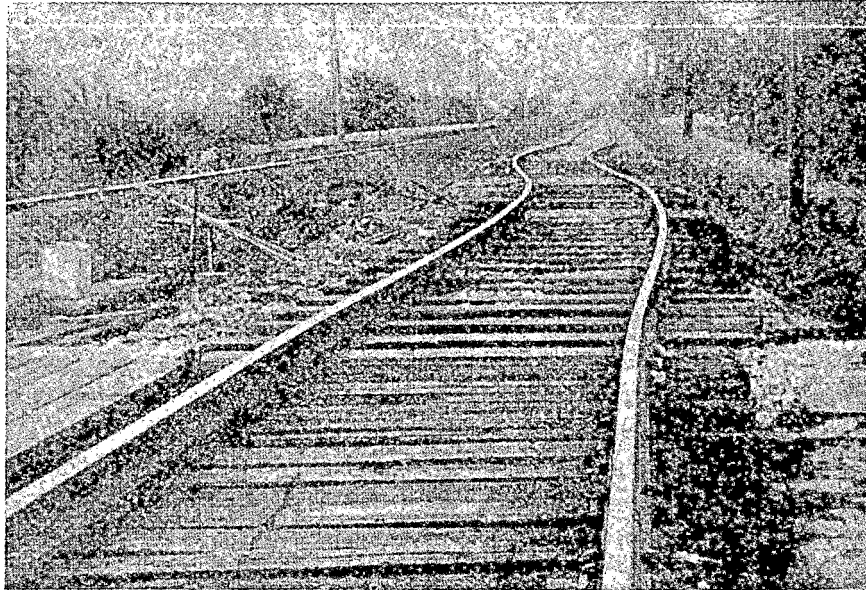
¹⁾ Numbers in brackets refer to references listed at the end of this report.

since World War II in the U.S.A. and abroad. However, this development has increased the occurrence of track buckling due to constrained thermal expansions.

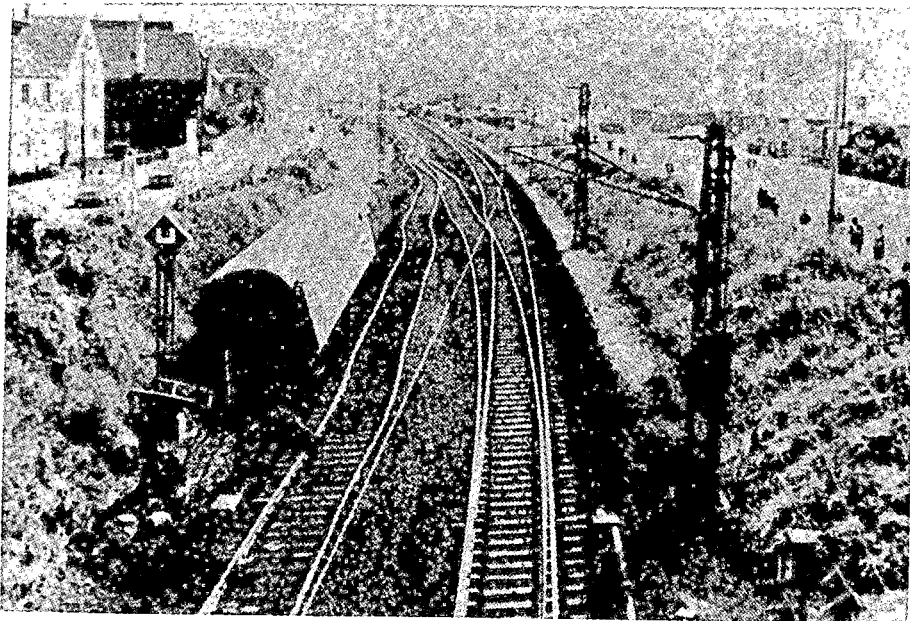
Examples of buckled tracks, jointed as well as welded, are shown in Fig. 1. In 1927, A. Wöhrl [2] reported that cases of buckling of conventional tracks came to his attention, although he could not find references to it in the literature. A detailed description of three derailments caused by buckled continuously welded tracks, which took place during hot summer days in 1969 in England, was presented in 1970 by C. F. Rose [3]. Descriptions of train derailments in the U. S., caused by thermal track buckling, are contained in various accident reports of the Office of Safety-Federal Railroad Administration (FRA).

Since the early nineteen thirties, many track stability analyses and results of track buckling tests were published. In spite of this extensive effort by many investigators and railroad research institutes, to date no generally accepted analysis is available for computing the buckling temperature of a railroad track ([4] p. 104).

A critical survey of the analyses of thermal track buckling and of related tests was recently presented by A. D. Kerr [5]. This survey revealed that the majority of the published calculations are not suitable for analyzing thermal track buckling problems, because they are based on formulations which do not describe correctly the physical problem under consideration. Those few analyses which are conceptually on the right path, exhibit analytical shortcomings with an unknown effect on the final results.



(Schweizerische Bauzeitung, 1925)



(About 1970, Courtesy Prof. J. Eisenmann, Munich, Germany)

FIG. 1 BUCKLED RAILROAD TRACKS

To eliminate some of these shortcomings, in 1976 A. D. Kerr presented an improved analysis for track buckling in the lateral plane [6]. The mathematical level of this analysis is, however, relatively high. In order to simplify its utilization, the final results were evaluated numerically for a wide range of track parameters and the obtained results were plotted as graphs. These results are presented in Section 4 of this report.

The purpose of the present report is to discuss the occurrence of axial forces in the rails due to changes in rail temperature, to discuss thermal buckling of straight tracks, to present a simple method for the analysis of thermal buckling, and to summarize some of the measures developed by various railroads for its prevention.

2. THE DISTRIBUTION OF RAIL COMPRESSION FORCES
CAUSED BY A UNIFORM TEMPERATURE INCREASE

As is well known, when a straight unconstrained rail of length L is subjected to a uniform temperature rise T_0 , its length increases by

$$\Delta L = \alpha L T_0, \quad (2.1)$$

where α is the coefficient of linear thermal expansion. If this elongation is prevented, as is the case in a long straight jointless track, a compression force

$$N_t = E A \alpha T_0 \quad (2.2)$$

builds up in the rails, as shown in Fig. 2. In eq. (2.2), E is Young's modulus of the rail material and A is the cross-section area of the two rails in a track.

A graphical presentation of the above equation, for $E = 2.1 \times 10^6$ kg/cm² (29.87×10^6 lb/in²) and $\alpha = 1.15 \times 10^{-5}$ 1/C^o, is shown in Fig. 3. For example, for a railroad track with 132 lb. rails and a uniform temperature increase in the rails of 50^oC (90^oF), the axial compression force induced in both rails is $P = 202$ tonnes (222 tons)¹⁾. This force may be sufficient to buckle the track. Note also that, for the same temperature increase, the axial force induced in a track increases with increasing rail weight (because of increasing area A), but the stress remains the same.

It should also be noted that, although during uniform heating (or cooling) of an infinitely long CWR the axial forces in the rails vary, the rails do *not* move axially.

¹⁾ Note: 1,000 kg = 1 tonne; 2,000 lb = 1 ton; and 1 tonne = 1.1023 tons.
The term kg means kilogram force.

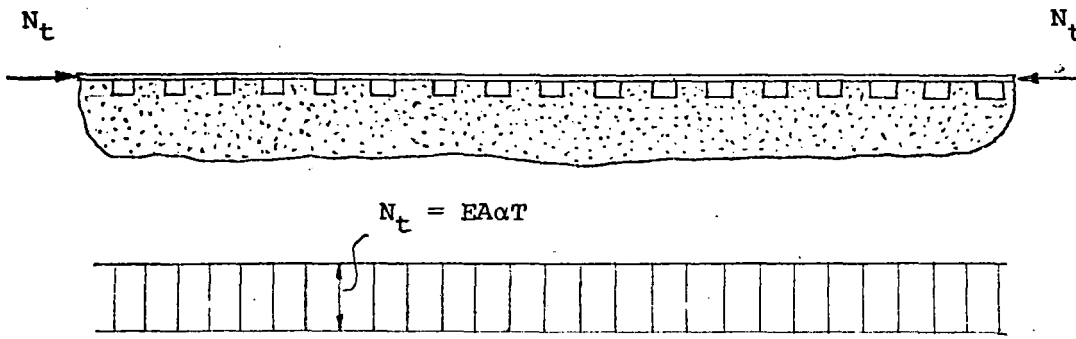


FIG. 2 AXIAL FORCE DISTRIBUTION IN THE RAILS OF A STRAIGHT JOINTLESS TRACK

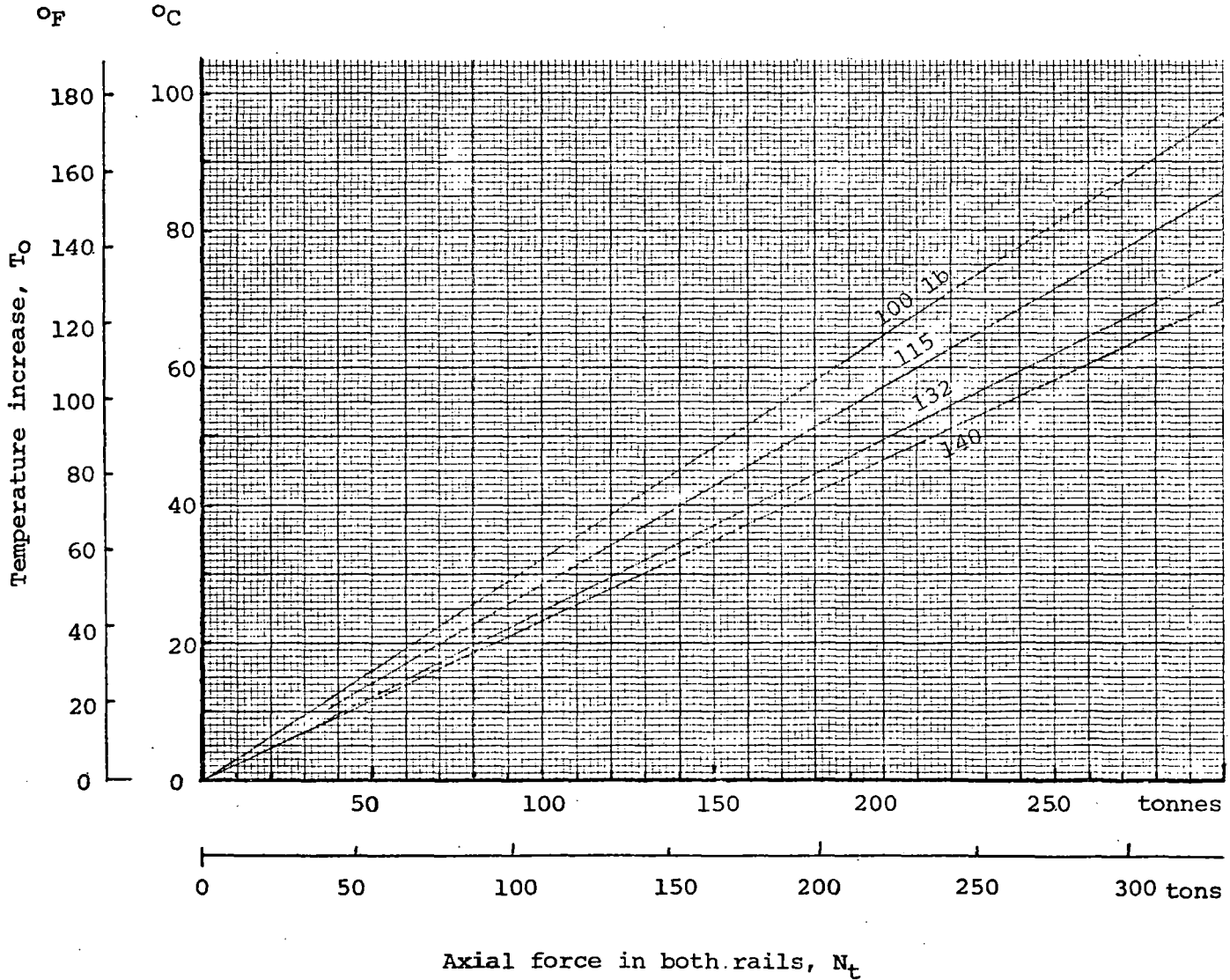


FIG. 3 RAIL TEMPERATURE INCREASE VS. AXIAL FORCE IN RAILS.

For the understanding of track buckling it is also necessary to establish the distribution of axial forces in a rail of finite length L , that is part of a track. When the *ends* of the rails are prevented from moving axially, the situation is the same as with very long rails. Namely, the axial force N_t is constant throughout the track section for a given temperature increase, and the rails do not move axially. Next consider the case when the rail *ends* are not constrained axially. If it is assumed that the axial resistance between the rail-tie structure and the ballast is constant¹⁾, say r_0 , then the axial force distribution in the rails (which are well anchored to the cross-ties) caused by a temperature increase T_0 is as shown in Fig. 4.

The end regions, where the axial force increases from zero to N_t , are referred to in the literature as the rail "breathing" regions. The distribution of the axial forces in these regions is determined from the free body diagram shown in Fig. 5. Equilibrium of forces in the axial direction yields

$$N(x) = r_0 x \quad (2.3)$$

Thus, N varies linearly. The length of the breathing region is determined from the condition that at $x=b$, the axial force is $N = N_t$. Substituting this condition into eq.(2.3) yields

$$b = N_t / r_0 \quad (2.4)$$

Note that b depends on r_0 and also on the magnitude of N_t , hence on the temperature increase T_0 , as indicated (by a dashed line) in Fig. 4.

¹⁾ Tests for the determination of the axial resistance r , will be described in Section 5.

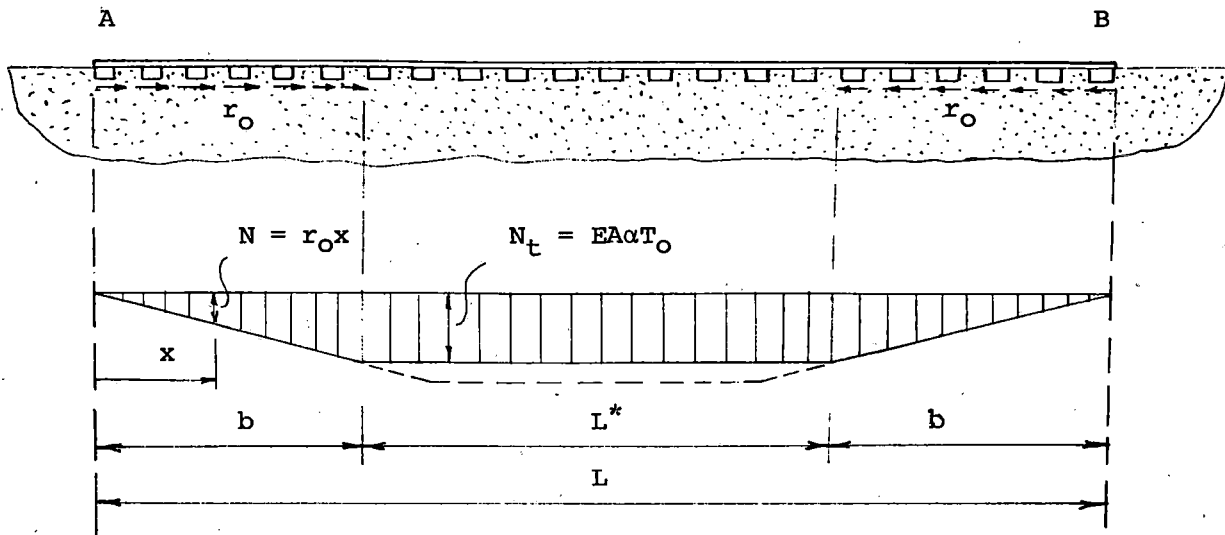


FIG.4 AXIAL FORCE DISTRIBUTION IN A TRACK OF LENGTH L
 (based on the simplifying assumption $r_0 = \text{const}$)

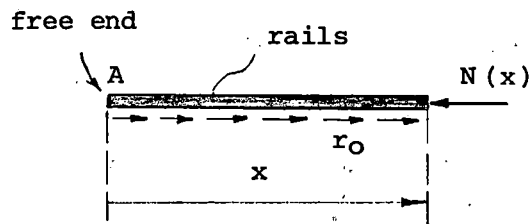


FIG.5 FREE BODY DIAGRAM FOR THE DETERMINATION OF THE
 AXIAL FORCE IN THE "BREATHING" REGION.

As example, consider a track of length $L = 800$ meters (2,625 ft) with continuously welded 132 lb rails. At both ends the track is free to expand axially. Assume that the rails are subjected to a temperature increase $T_0 = 50^\circ\text{C}$. As shown before, the corresponding axial compression force is $N_t = 202$ tonnes (222 tons). With $r_0 = 800$ kg/m (538 lb/ft), it follows from eq.(2.4) that the corresponding b is 252 meters (828 ft). Thus, for the problem under consideration, the distribution of the axial forces will be as shown in Fig. 4, with $b = 252$ meters (828 ft) and $L^* = 296$ meters (970 ft).

From Fig. 4 it follows that for any rail length L larger than $2b$, the *largest* axial force takes place in the L^* region and is equal to N_t . Therefore, in the above track example, whether the rail length is 800 meters or 8,000 meters, the largest axial compression force due to $T_0 = 50^\circ\text{C}$ will be the same, namely $N_t = 202$ tonnes. It is essential to realize this situation when considering the possibility of track buckling and when assessing the need to include expansion joints in C W R's.

From Fig. 4 it also follows that, in order to limit the largest compression force in a track rail, for an anticipated temperature increase T_0 , the rail length L has to be smaller than the corresponding $2b$.

It should also be noted that the axial movements caused by temperature variations are confined to the "breathing" regions. Thus, the inner part of the rail strand of length L^* neither expands nor contracts. In the example discussed above ($T_0=50^\circ\text{C}$), the rail ends will move by the same amount whether the rail length is 800 or 8,000 meters.

The corresponding displacement of each rail end is

$$u_0 = \frac{r_0 b^2}{2EA} = \frac{\alpha T_0 b}{2} = \frac{(EA\alpha T_0)^2}{2r_0 EA}, \quad (2.5)$$

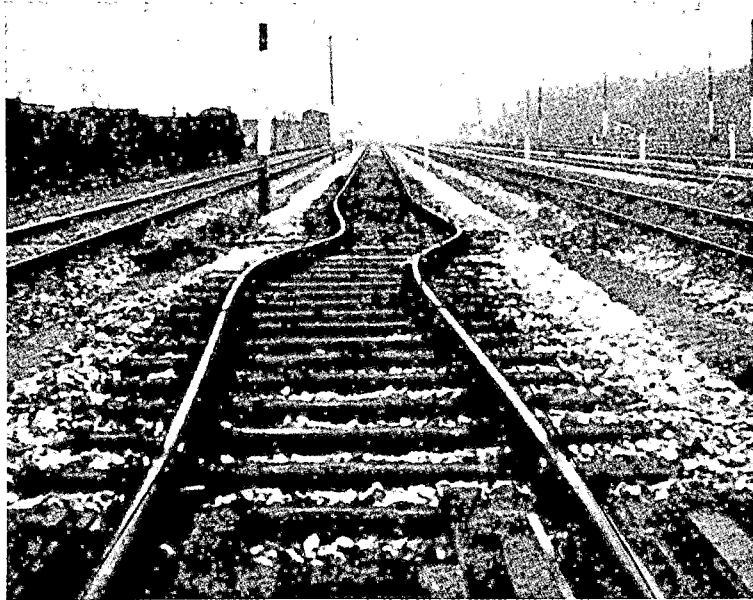
where A is area of both rails. Thus, for a temperature increase $T_0 = 25^\circ\text{C}(77^\circ\text{F})$ the end displacement is 1.8 cm (0.7 in).

3. RESULTS OF THERMAL TRACK BUCKLING TESTS

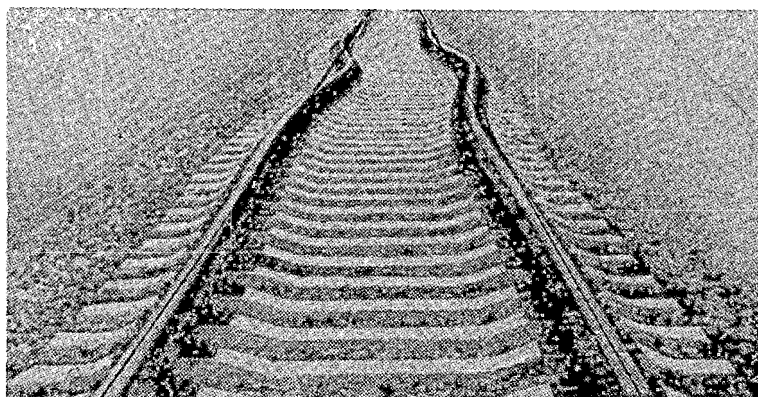
In the early track buckling tests by O. Ammann and C. v. Gruenewaldt [7] and by J. Nencsek [8], hydraulic jacks were utilized to induce compression forces in the rails of a track. As shown by A. D. Kerr in References [5] and [9], this is generally not a suitable method for simulating thermal compression forces (in particular during buckling) and hence the results obtained in [7] and [8] are of questionable value for the determination of track buckling temperatures.

In later track buckling tests (since about 1934) conducted by various railroads, the axial forces were induced by heating the rails. Their test set-ups consisted of a track section whose movements were constrained at both ends by two heavy concrete piers [10, 11, 12] or by locomotives which were placed on both ends of the test section [13,14,15]. In all these tests the heated track section buckled laterally like heated tracks in the field, as shown in Fig. 1. A survey of these tests and a discussion of the obtained test results is presented in Reference [5]. Typical buckling modes observed in those tests are shown in Fig. 6. Certain results of these tests, necessary for the understanding of thermal track buckling, are described below.

Results of a series of track buckling tests conducted for the Federal German Railways (DB) were reported by F. Birmann and F. Raab [10] in 1960. The test facility was located at the Technical University of Karlsruhe. The track section was 46.50 meters (153 ft) long and was confined at both ends by reinforced concrete blocks (624 tonnes each), as shown in Fig. 7. The axial compression force in the rails was induced by electric resistance heating. A total of 21 tests were conducted.



(a) Nearly antisymmetrical buckling mode [7].



(b) Nearly symmetrical buckling mode [12].

FIG. 6 BUCKLING MODES OBSERVED IN TESTS

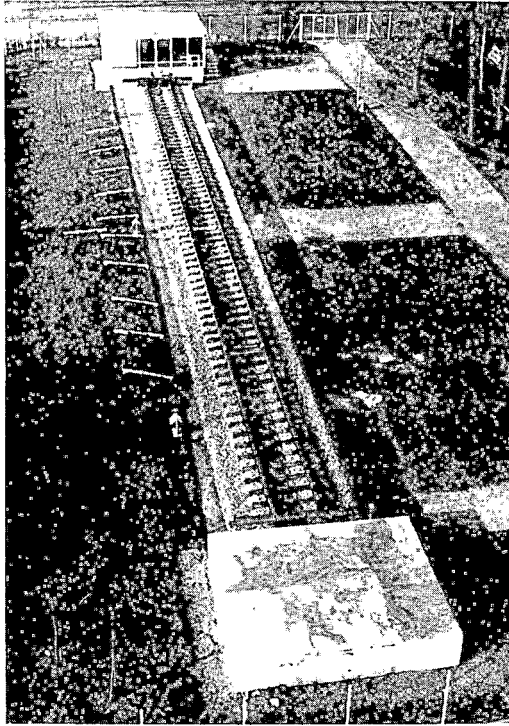
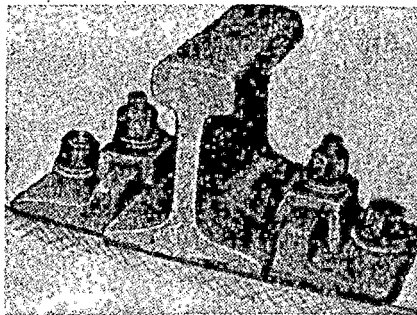
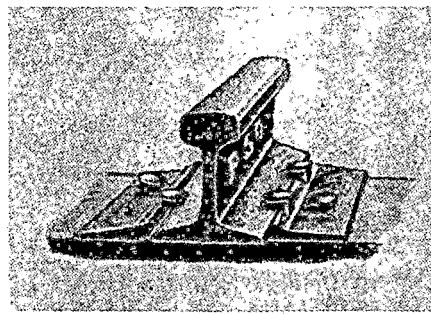


FIG. 7 THE TRACK BUCKLING FACILITY AT KARLSRUHE [10]



(a) K-type fastener



(b) Cut-spike fastener

FIG. 8 RAIL-TIE FASTENERS USED IN TEST TRACKS

The wooden cross-tie track K49 (Hh) was used in 12 tests. This track consisted of S49 rails attached to wooden cross-ties by means of K-fasteners, as shown in Fig. 8a. The tie spacing was 62.5 cm (21.5 in). To simplify comparisons, the essential properties of the rails used are listed in Appendix A. Note that the lateral stiffness of the S49 rail ($I = 320 \text{ cm}^4 = 7.66 \text{ in}^4$) is less than the stiffness of the 115 lb rail.

In all tests [10], the track buckled laterally. The buckling modes exhibited 2, 3, or 4 noticeable half-waves. It was observed that a typical half-wave was about 5 to 6 meters (16 to 20 ft) long and the largest amplitude of lateral displacement was about 25 centimeters (10 in).

For the twelve track tests with wooden ties, K49(Hh), buckling took place for temperature increases $65 \text{ }^\circ\text{C} < T_0 < 140 \text{ }^\circ\text{C}$. The measured axial compression forces (in both rails) ranged from 177 tonnes (195 tons) to 340 tonnes (375 tons).

Birmann and Raab [10] observed that the straight tracks, which did not exhibit noticeable imperfections, buckled at much higher temperature increases than those tracks with noticeable lateral imperfections. They also observed that buckling of "straight" tracks occurred suddenly, with a loud bang, whereas the imperfect tracks buckled gradually and quietly. This response characteristic is very important and has to be taken into consideration when choosing the analytical formulation for lateral track buckling [6]. This feature will be discussed further in Section 4.

Birmann and Raab [10] also observed that by using different fasteners in some tests, the corresponding buckling load differed by as much as 25%.

A very extensive series of track buckling tests was conducted at the Central Railroad Research Institute (CNII) in the USSR. A description of these tests and a discussion of the obtained results is contained in a book by E. M. Bromberg [12] published in 1966. The test stand for straight tracks was 100 meters (328 ft) long. The track section was mounted between two concrete piers. The compression force in the track was induced by electric resistance heating.

The tested tracks consisted of jointless P50 or P65 rails on wooden or reinforced concrete ties using a variety of fasteners. Many of the tests were conducted with weakly compacted ballast in order to simulate the conditions of newly constructed or renovated tracks. In all tests the tracks buckled in the horizontal plane, exhibiting 3, 4, or 5 half-waves of the type shown in Fig. 6.

In order to simplify comparisons with U. S. tracks, the essential properties of the tested rail sizes are given in Appendix A. Note that the P50 rail is about 16% less stiff laterally than the 115 lb rail ($I = 9.05 \text{ in}^4$ versus 10.8 in^4) and that the P65 rail is slightly less stiff than the 132 lb rail ($I = 13.7 \text{ in}^4$ versus 14.6 in^4).

During tests in which the temperature was continuously increased, it was observed that up to an increase, say T_1 , there were no noticeable displacements. For $T_0 > T_1$ the track started to deform laterally. The rate of deformation increased with increasing T_0 . At a temperature increase $T_0 = T_2$, the track buckled. The corresponding load displacement

graph is shown in Fig. 9(a). It is similar to the one observed by Birmann and Raab ([10], Fig. 16).

During a number of these tests it was observed that when a track was heated by a temperature increase $T_1 < T_0 < T_2$, at which lateral displacements occurred, and subsequently the rail temperature was lowered to $T_0 < T_1$, the lateral displacements did not vanish, as shown in Fig. 9(b). Pointing out that an actual track is usually exposed during the summer to hot days followed by cool nights, Bromberg suggested that the resulting temperature variations ($T_0 \geq T_1$) may cause an accumulation of undesirable *permanent* lateral track deformations, for temperature increases which do not cause actual track buckling.

Citing the need for improved ride quality and for reduced track maintenance, Bromberg suggested that the admissible temperature increase be smaller than T_1 (thus $T_0 < T_1$), as a desirable criterion for the design of welded tracks. In order not to restrict unduly the admissible temperature increase T_0 (beyond neutral), Bromberg modified this criterion to

$$T_0 < T_1^* \quad (3.1)$$

where T_1^* is the temperature increase which causes a lateral displacement of 0.2 mm for a straight track (as shown in Fig. 9a) and 0.4 mm for a curved track. For additional comments on this approach to track stability, refer to Reference [4] (Part II, §3).

Of special interest for U. S. tracks are the test results obtained on track sections with P50 rails, wooden ties (1840 per km, thus center-to-center tie spacing of 54.3 cm = 21.4 in), and cut-spike fasteners of the type shown in Fig. 8b. Results for two of these tests are given in Table 1.

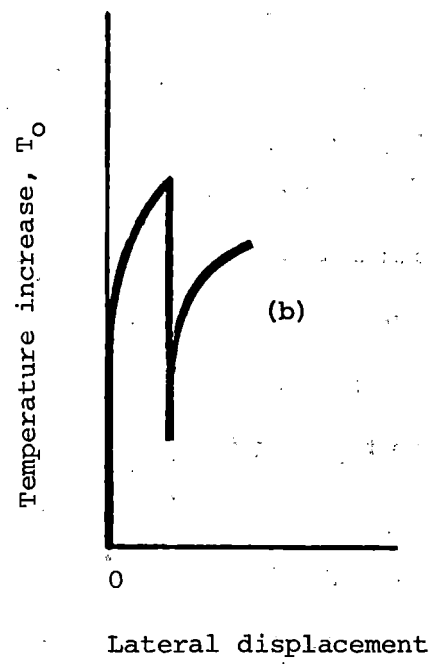
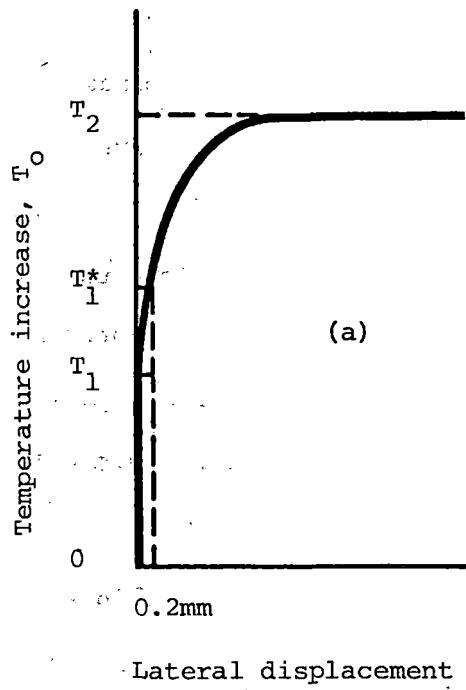
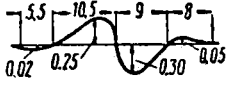
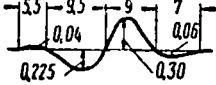


FIG. 9 TEMPERATURE INCREASE VS. LATERAL DISPLACEMENT OBSERVED IN TRACK BUCKLING TESTS.

TABLE 1: TEST RESULTS FOR P50 TRACK SECTIONS WITH WOODEN TIES AND CUT-SPIKE FASTENERS (Ref. [12] p. 29)

Test No.	Temperature increase in °C (°F)		Corresponding axial force in tonnes (tons)		Deflected shape in lateral plane (dimensions in meters)
	T ₁ [*]	T ₂	N ₁ [*]	N ₂	
15	52 (94)	73 (131)	170 (187)	238 (262)	
17	59 (106)	69 (124)	193 (212)	225 (248)	

(Note: $N_1^* = EA\alpha T_1^*$ and $N_2 = EA\alpha T_2$, where A is area of both rails)

According to Ref. [12], the above results fall within the range recorded in the tests with the same track section but with K4 fasteners ($N_1^* = 150$ to 196 tonnes, and $N_2 = 200$ to 240 tonnes).

The K4 fastener (of the type shown in Fig. 7a) is generally considered to be a more rigid fastener than the cut-spike fastener. Therefore, one would expect the buckling temperatures to be higher for the track with K4 fasteners. One reason why this is not the case for the above test results could be that the cut-spike track sections were specially prepared for these tests and were not exposed to the rolling stock prior to buckling. As it is well known, moving trains have a tendency to loosen the connection between the cut-spike and the ties, which results in a reduction of the fastener rigidity also with respect to the vertical axis. This suggests that for an *actual* track with cut-spike fasteners, the buckling temperatures will be lower than those shown in Table 1 (assuming that the lateral resistance of the ballast and the other track properties remain essentially unchanged).

For additional test results the reader is referred to References [10-15]. For a discussion of some of these test results refer to [5].

The effect of test track *length*, on the obtained results, is analysed and discussed in a recent paper by Kerr [16].

4. ANALYSIS OF THERMAL TRACK BUCKLING

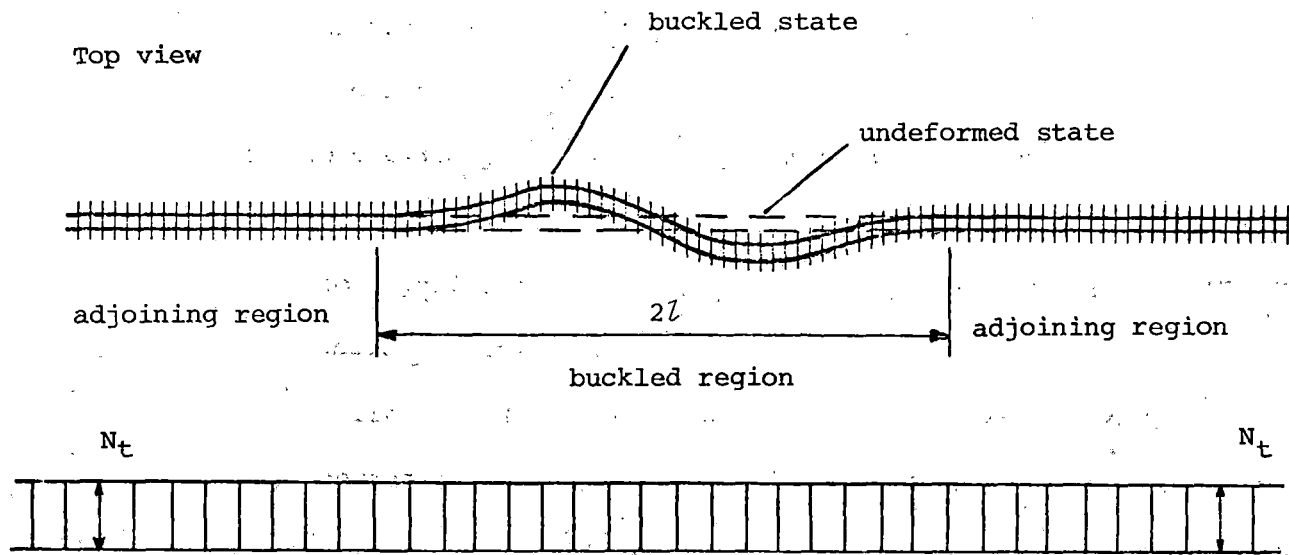
A critical survey of the analyses of thermal buckling of straight tracks was presented in 1975 by Kerr [5]. This survey revealed that the majority of the proposed analyses are conceptually incorrect and hence unsuited for analyzing thermal track buckling problems.

One error made by several authors was the assumption that the railroad track may be represented by an elastic beam which is continuously attached to a linear Winkler foundation before and during buckling. Another shortcoming was the failure by a number of authors to take into consideration the drop of the axial force in the buckled region.

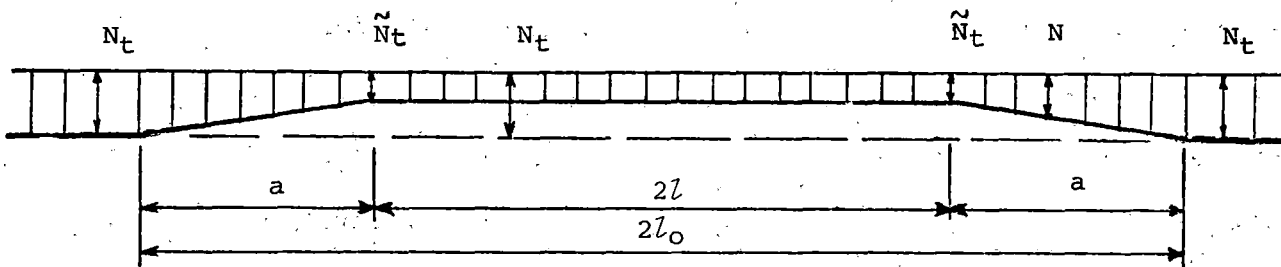
Those few analyses which are conceptually on the right path exhibit analytical shortcomings, with an unknown effect on the final results. To eliminate some of these shortcomings, in 1976 Kerr presented a new improved analysis for thermal buckling of straight tracks [6].

The developed analysis is based on the observation that the buckling mode of a long straight track takes place usually in the lateral plane and that it consists of a *buckled region* which exhibits relatively large lateral deformations and two *adjoining regions* which appear to deform only axially, as shown in Fig. 10. In the buckled region, a part of the constrained thermal expansions is released, which results in a reduction of the axial force. In the adjoining regions, because of the ballast resistance to axial displacements of the rail-tie structure, the constrained thermal expansions vary, and so does the axial force.

In this analysis, the rail-tie structure was replaced by an equivalent beam of uniform cross-section consisting of the two separate rails each deforming axially and in bending. This assumption, which neglects



(a) Axial compression force before buckling



(b) Axial compression force after buckling

(Note that in an actual track a is several times larger than l)

FIG. 10 DISTRIBUTION OF AXIAL COMPRESSION FORCES BEFORE AND AFTER BUCKLING

the torsional rigidity of the fasteners, appears justified for the tracks currently used in the USA. When the fastener rigidity is not negligible, the resulting "safe temperature increase" is higher. Thus, the corresponding results obtained in Reference [6] are on the safe side.

The *lateral resistance* exerted by the ballast on the rail-tie structure (due to lateral displacements) consists of the friction forces between the ballast and the bottom surface and the two long sides of the ties, as well as of the pressure the ballast exerts against the front surface of the ties, as shown in Fig. 11(a). For the developed analysis it was assumed that the resulting lateral resistance is $\rho_0 = \text{const}$ (per unit length of track axis). The justification for this assumption is suggested in Reference [17].

The *axial resistance* exerted by the ballast on the rail-tie structure (due to axial displacements) consists of the resistance between the ballast and the bottom surface of the ties, and the pressure on the vertical tie surfaces exerted by the ballast in the cribs, as shown in Fig. 11(b). For the developed analysis it was assumed that the resulting axial resistance is $r_0 = \text{const}$ (per unit length of track axis).¹⁾

Furthermore, it was assumed that both track rails are subjected to a *uniform* temperature increase T_0 , above installation (neutral) temperature, and that prior and during buckling the response of the rail-tie structure is *elastic*.

Typical equilibrium branches for a perfectly straight track, based on the above assumptions, are shown in Fig. 12. Note that each point on the equilibrium branch corresponds to an equilibrium configuration of the track: Branch I corresponds to the straight unbuckled equilibrium states and branch II to the laterally deformed configurations.

1) The effect of this assumption is determined in a forthcoming report "An improved analysis for thermal track buckling" by A. D. Kerr.

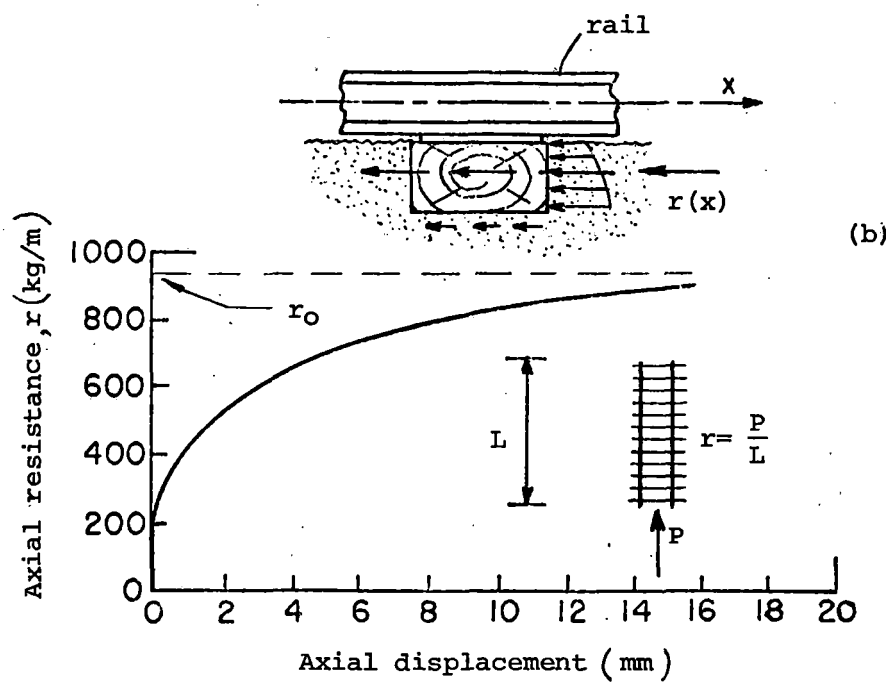
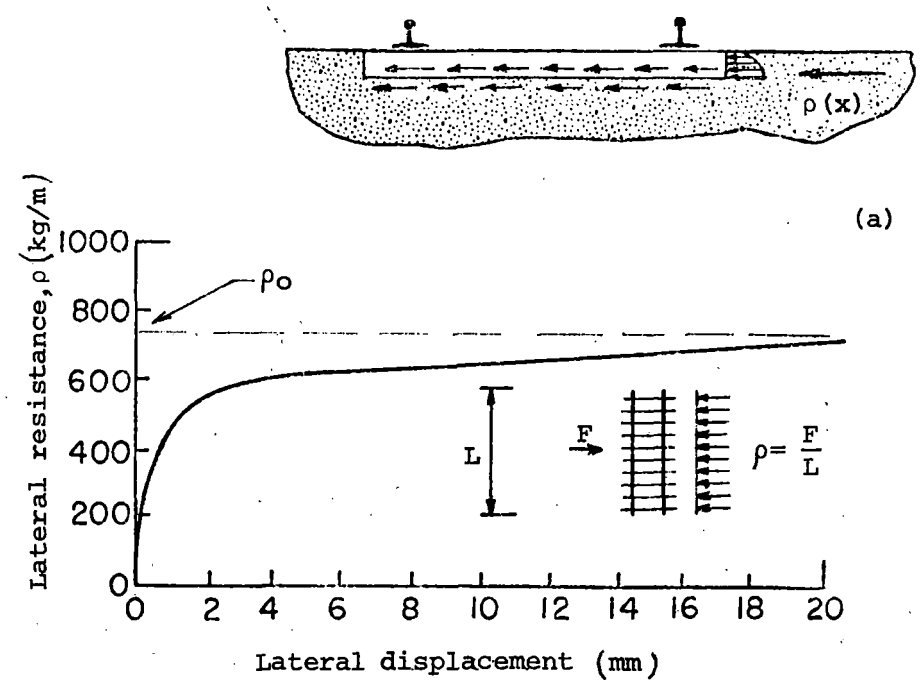


FIG. 11 RESISTANCES BETWEEN RAIL-TIE STRUCTURE AND BALLAST

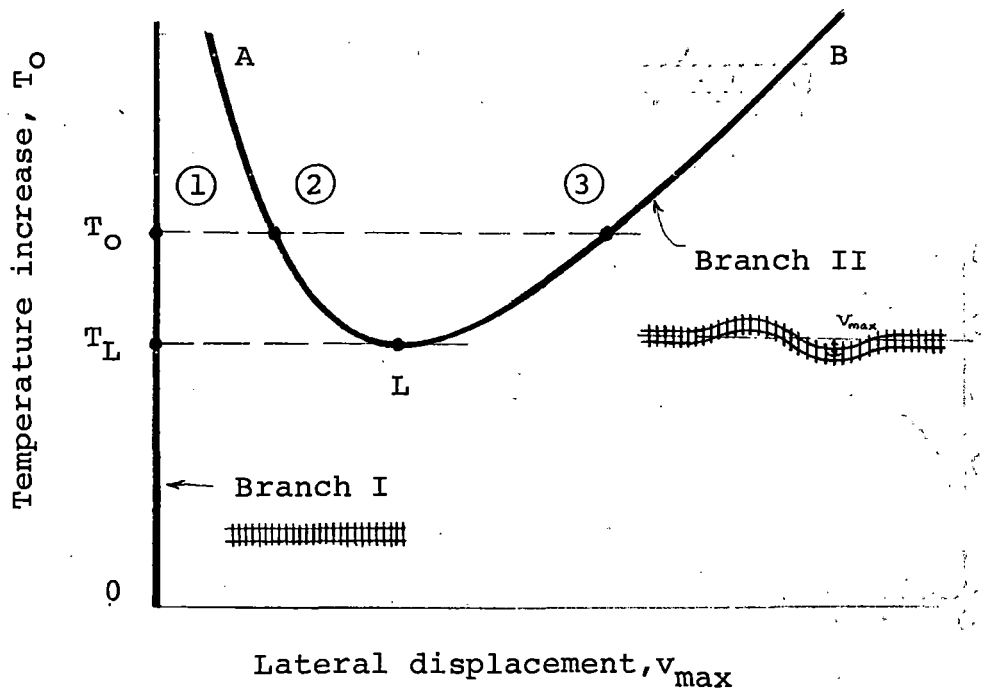


FIG.12 TYPICAL EQUILIBRIUM BRANCHES FOR A HEATED STRAIGHT TRACK

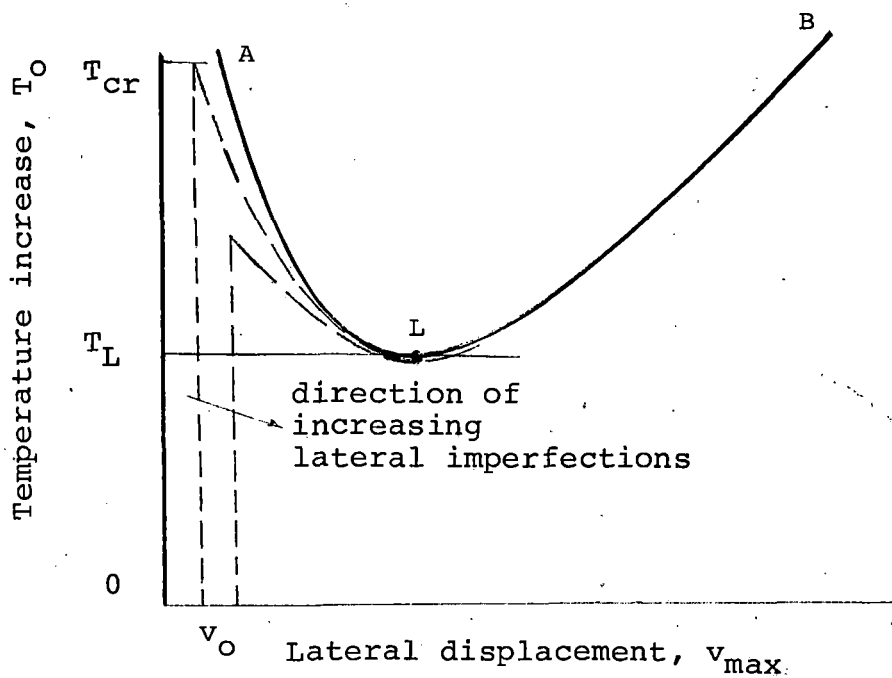


FIG.13 TYPICAL EQUILIBRIUM BRANCHES FOR A TRACK WITH LATERAL GEOMETRIC IMPERFECTIONS

According to Fig. 12, when the track is subjected to a temperature increase $T_0 < T_L$ there exists only the straight equilibrium configuration. For such a T_0 , when the track is pushed sideways at a point it will return to its original straight position once the lateral load is removed (assuming that the track response is elastic). Note, however, that to a temperature increase $T_0 > T_L$ there correspond three states of equilibrium: The (stable) straight state (1), the (unstable) configuration (2) on branch AL, and the (stable) configuration (3) on branch LB [9]. Thus, when the straight track buckles at a temperature increase $T_0 > T_L$, it will move to the laterally deformed equilibrium configuration (3) on branch LB.

From the above discussion it may be concluded that a *temperature increase* for a straight track is *safe against buckling* when

$$T_0 < T_L . \quad (4.1)$$

Because railroad tracks are usually not "perfectly" straight, it is necessary to know the effect of geometric imperfections on the track response. The corresponding equilibrium branches [9,17] for relatively small lateral track imperfections are shown schematically, as dashed lines, in Fig. 13. Note that the T_L -value for each of these branches is very close to the T_L -value of the perfectly straight track. Hence, the criterion stated in (4.1), with a T_L -value for a "straight" track, is also valid for a track with small lateral imperfections.

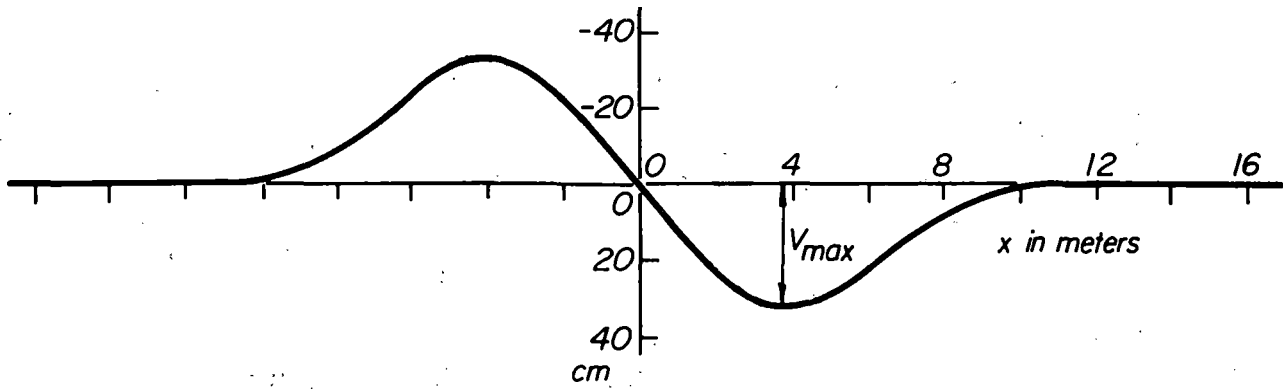
It should be noted, that when the geometrically imperfect rails are heated and T_0 reaches the value T_{cr} , the track will buckle sideways and will adopt an *equilibrium* configuration on branch LB. The buckling phenomenon itself is *dynamic* in nature, and hence is not included in these graphs (which show equilibrium curves). Note that with increasing imperfections T_{cr} , and hence v_{max} , decrease. It may be shown that the energy release also decreases. These findings agree with observations made by Birmann and Raab [10], as described in Section 3.

A *buckling analysis* of a railroad track subjected to thermal compression forces consists of two parts: (1) the determination of all equilibrium states and (2) the inspection of the determined equilibrium states to establish which are stable and which are not. The above discussion suggests that the *safe temperature increase* for preventing track buckling may be determined solely from the *post-buckling equilibrium* branches. This concept was adopted in Reference [6] and is used in the following.

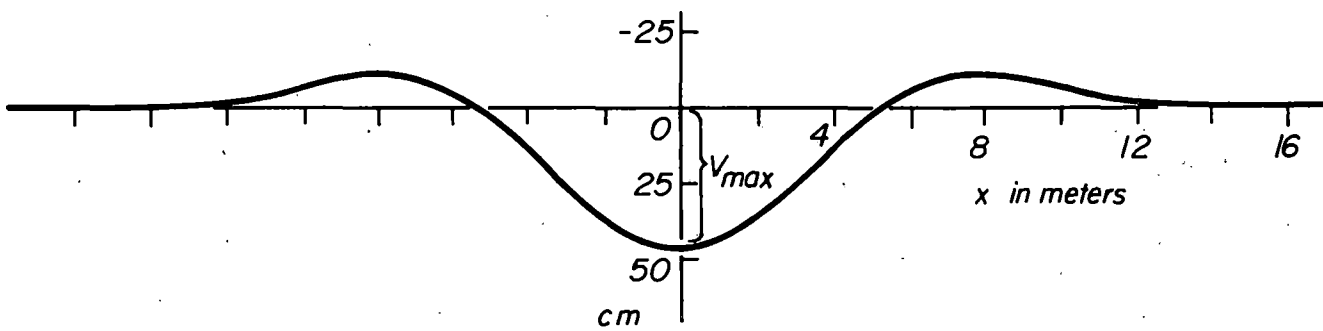
To insure an analytical formulation that is mechanically reasonable and mathematically consistent, the *equilibrium equations* for the rail-tie structure were derived by utilizing the nonlinear theory of elasticity and the principle of virtual displacements. To avoid the difficulties encountered by other investigators, when matching track regions which are governed by different differential equations and whose matching points are not fixed a priori along the track axis, use was made of variational calculus for variable matching points [18].

The typical buckling modes shown in Fig. 6 suggested the analysis of antisymmetrical and symmetrical buckling shapes. The analyses for the shapes, shown in Fig. 14, are contained in Reference [6]. In the following, only the results of their numerical evaluation are presented and discussed.

As example, the results of the numerical evaluation for a 132 lb track with $r_o = 1000$ kg/m (672 lb/ft) and $\rho_o = 900$ kg/m (605 lb/ft) are shown in Fig. 15. The solid line corresponds to the antisymmetrical S-shape (Mode II in Reference [6]). The dashed line corresponds to the symmetrical deformation shape (Mode III in Reference [6]).



a) Antisymmetrical mode



b) Symmetrical mode

Fig. 14 BUCKLED TRACK SHAPES OBTAINED FROM ANALYSIS FOR $T_0 = 50^\circ\text{C}$ (90°F)
 FOR $r_0 = 1000\text{kg/m}$ and $\rho_0 = 900\text{ kg/m}$.

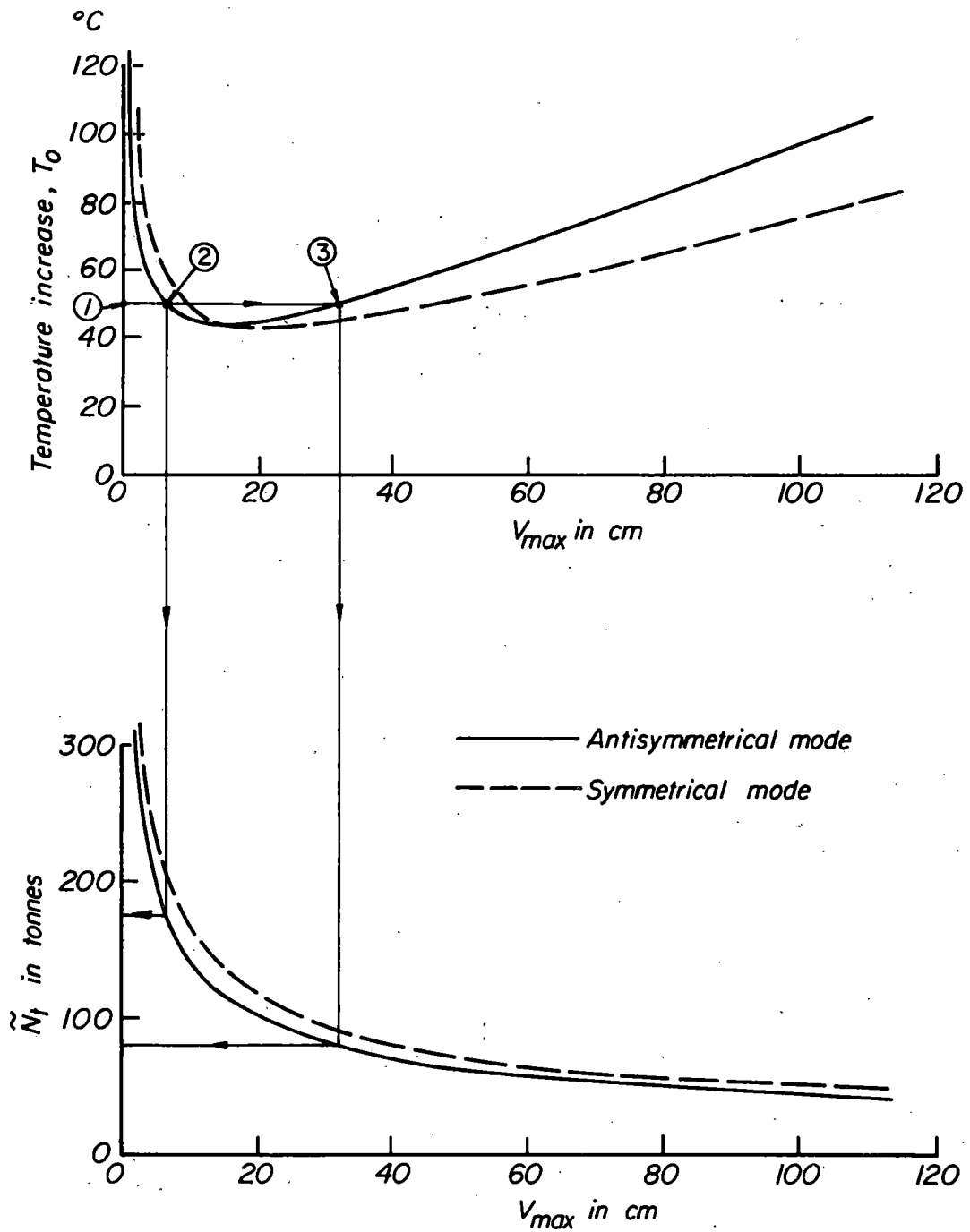


FIG. 15 EQUILIBRIUM BRANCHES AND CORRESPONDING AXIAL FORCE CURVES OBTAINED FROM ANALYSIS.

According to Fig. 15, for the above track and the S-shape, the *safe temperature increase* is $T_L \approx 43.5^\circ\text{C}$ (78°F). Note also that if the track should buckle for a temperature increase $T_0 = 50^\circ\text{C}$, then it will come to rest at the equilibrium configuration ③ on branch LB with the largest lateral deflection $v_{\max} = 32$ cm (12.5 in). The corresponding axial compression forces are: In the straight equilibrium configuration ① $N_t = EA\alpha T_0 = 202$ tonnes, in the *stable* equilibrium configuration ③ $N_t = 80$ tonnes. Thus, for a rail temperature increase of $T_0 = 50^\circ\text{C}$, the axial track force drops, due to buckling, to less than a half of its original value. For $T_0 = 60^\circ\text{C}$ the thermal force $N_t = 242$ tonnes drops to 65 tonnes; about a quarter of its original value. This finding contradicts the assertions made by various authors that the drop of the axial force is negligible.

According to Fig. 15, for a given track, also the magnitude of v_{\max} depends upon the temperature increase T_0 at which buckling will take place. To show this point, the corresponding values are presented in Table 2.

TABLE 2. DEPENDENCE OF v_{\max} and \tilde{N}_t ON T_0 , FOR THE 132 lb TRACK

T	$^\circ\text{C}$	43.5	45	50	60	70	80
v_{\max}	cm	15	22	32	48	63	78
N_t	tonnes	175	181	202	242	282	323
\tilde{N}_t	tonnes	115	96	80	65	57	52
\tilde{N}_t	% of N_t	66%	53%	40%	27%	20%	16%

Note that v_{\max} and \tilde{N}_t depend also on the track parameters, especially the resistances r_0 and ρ_0 .

Comparing the equilibrium branches in Fig. 15, it follows that the T_L values, for the symmetrical and antisymmetrical deformation modes, are almost the same, whereas the v_{\max} value for the symmetrical mode is larger (about 50%).

Note also that, for the range of temperature increases shown, the drop of the axial force due to buckling is about the same for both modes of deformation. For example, for $T_0 = 50^\circ\text{C}$ the axial force in the straight state (according to Fig. 2) is $N_t = 202$ tonnes whereas the corresponding \tilde{N}_t values for the stable deformed state ③ are about 80 tonnes each.

The antisymmetrical and symmetrical track shapes which correspond to the temperature increase $T_0 = 50^\circ\text{C}$ are shown in Fig. 14.

In order to establish the effect of *rail section* and *ballast condition* on the post-buckling track response, especially on the *safe temperature increase* T_L , the solutions presented in Reference [6] were numerically evaluated for the standard rail steel constants

$$\begin{aligned} E &= 2.1 \times 10^6 \text{ kg/cm}^2 = 3 \times 10^7 \text{ lb/in}^2, \\ \alpha &= 1.15 \times 10^{-5} \text{ 1/C}^\circ, \end{aligned} \tag{4.2}$$

and a range of track parameters. The graphs for the often utilized 132 lb rails and the S-shape of deformation are shown in Fig. 16 and Fig. 17. The effect of rail size and of the tie-ballast resistances r_0 and ρ_0 on the safe temperature increase T_L were calculated and are summarized in Fig. 18.

The graphs in Fig. 18 were obtained for the antisymmetrical S-shape of deformation. The corresponding graphs for the symmetrical deformation shape were found to be very close to those of the S-shape. Therefore, for engineering purposes, *the graphs in Fig. 18 may be considered valid for both modes of deformation.*

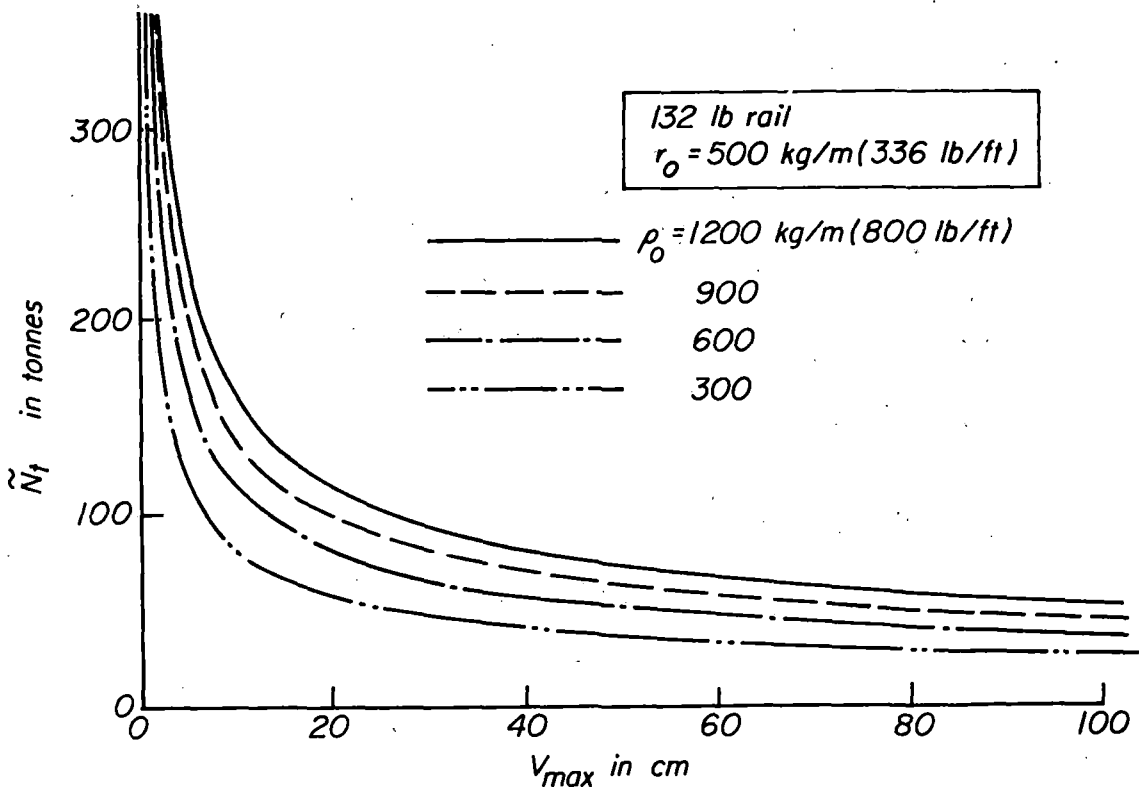
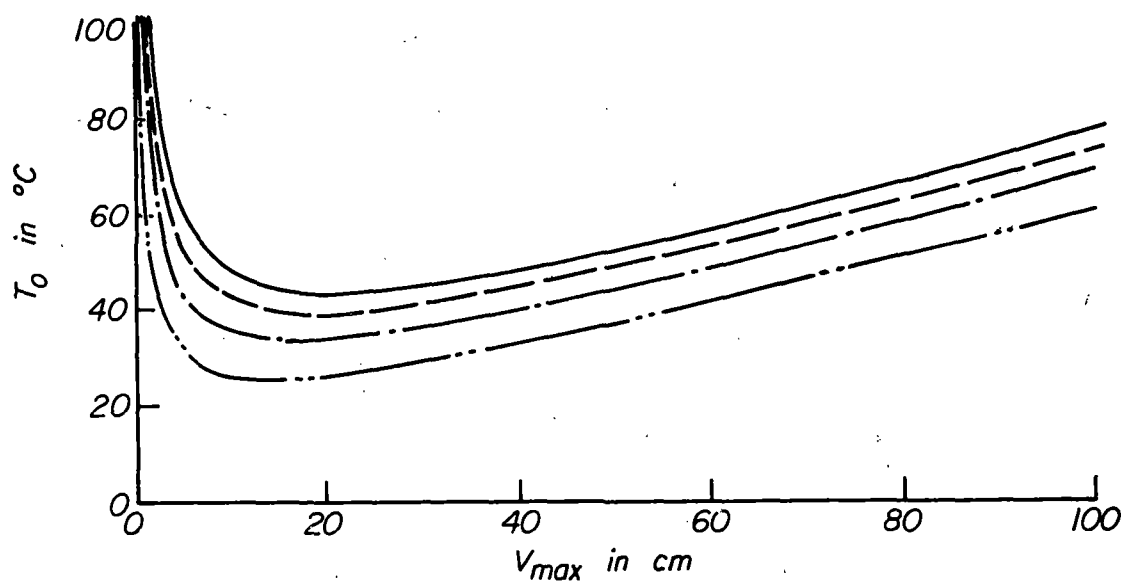


FIG. 16 EQUILIBRIUM BRANCHES FOR 132 lb TRACK FOR VARIOUS VALUES OF RAIL-TIE BALLAST RESISTANCE.

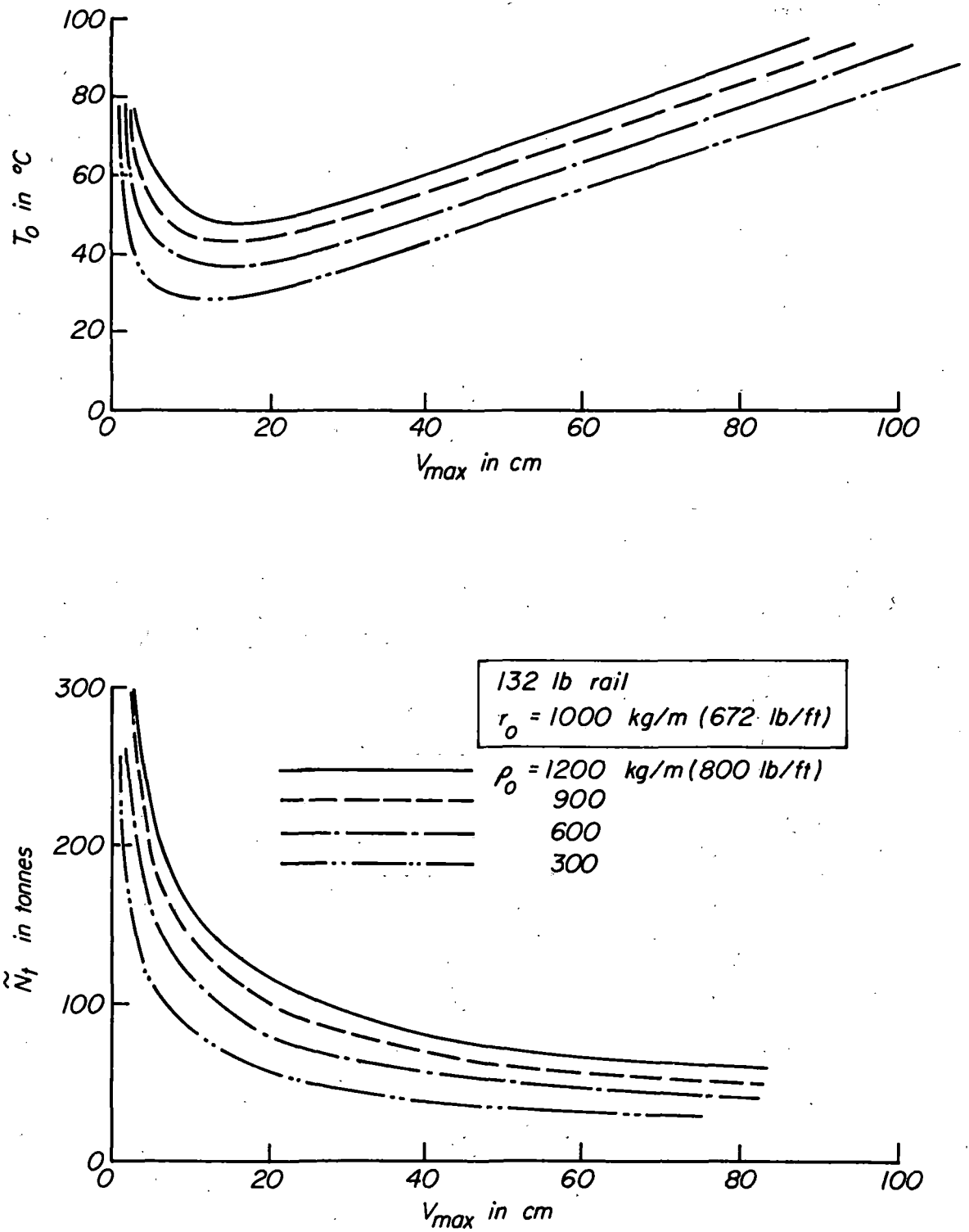


FIG. 17 EQUILIBRIUM BRANCHES FOR 132 lb TRACK FOR VARIOUS VALUES OF RAIL-TIE BALLAST RESISTANCE.

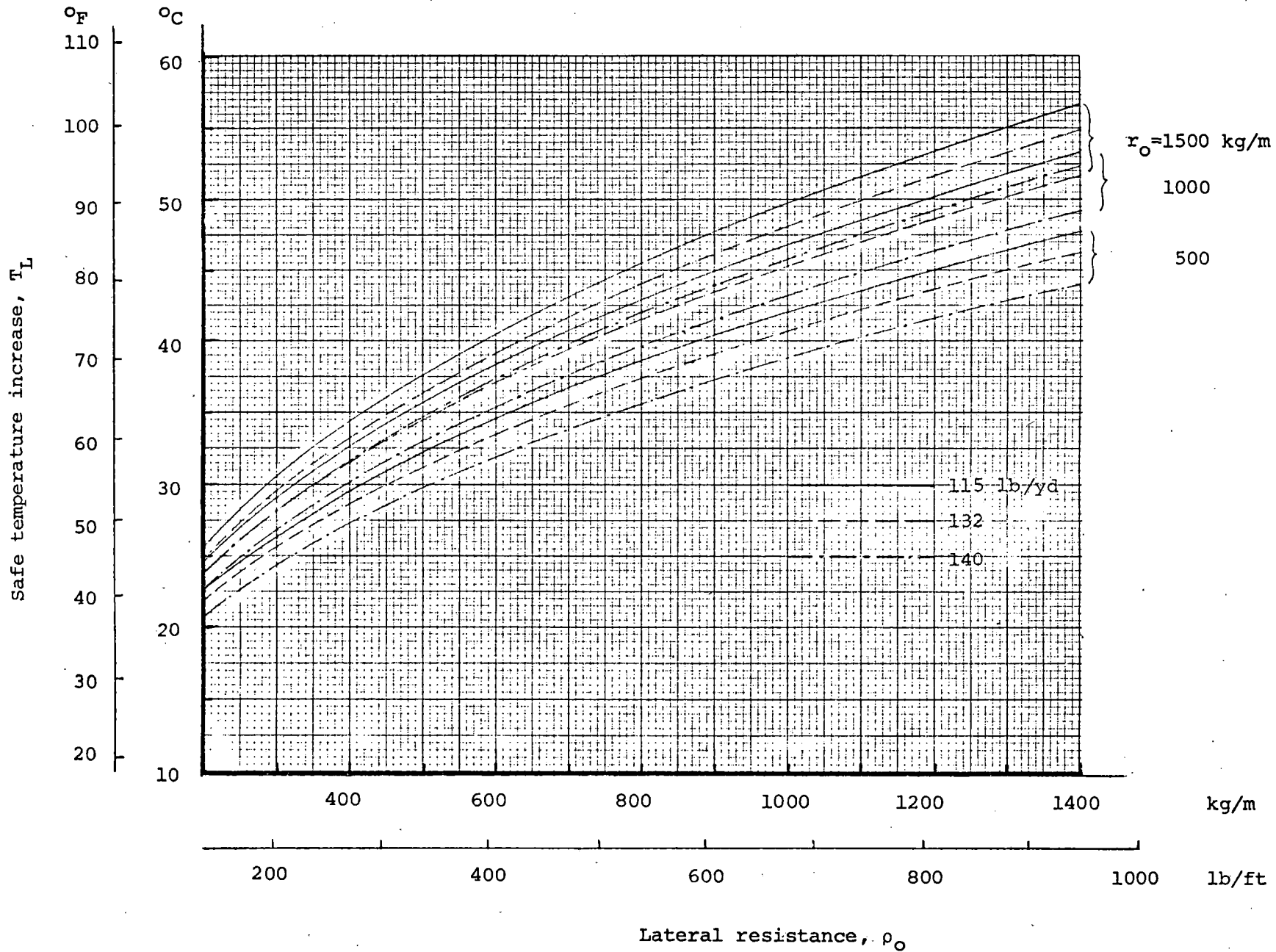


FIG. 18 DEPENDENCE OF SAFE TEMPERATURE INCREASE T_L ON TRACK PARAMETERS

5. THE TRACK PARAMETERS NEEDED FOR THE PRESENTED ANALYSIS

The graphs in Figs. 14 to 18 are based on the E and α values for rail steel, given in (4.2). The use of these graphs for analyzing track buckling requires also the knowledge of the track parameters A , I , ρ_0 , r_0 . As pointed out in the previous section, A and I are the geometric properties of the rail cross-section; A is the cross-sectional area of both rails and $I = 2I_r$ is the moment of inertia of both rails with respect to their vertical centroidal axes. These values are listed for various rail types and sizes in Appendix A. Note, however, that if the rails of a track to be analysed are excessively worn, then the listed A and I values have to be reduced accordingly.

The meaning of r_0 and ρ_0 was also defined in the previous section. These parameters are determined by means of field and/or laboratory tests, in which a rigidized track panel is moved axially or laterally by an increasing force and then the corresponding load-displacement values are recorded, as shown in Fig. 11. r_0 or ρ_0 is the resistance value for which the corresponding curve levels off.

When choosing the *length* of the track test panel, note that the r_0 , ρ_0 values to be determined be such that the analytically obtained values (T_L , \tilde{N}_t , v_{\max} , etc.) be as close as possible to the actual quantities in the field. To achieve this objective the length of the test panel has to be sufficiently long, say 10 meters (32 feet).

The use of only one tie, for the determination of r_0 or ρ_0 , appears to be inadmissible. The reasons are similar to those presented in Reference [19] Section 3, in connection with the determination of the track modulus in the vertical plane. Namely, in tests of this type one tie responds differently in the ballast base than do the closely spaced ties of a long panel.

Furthermore, because of the granular character of the ballast, the loading of one tie at different locations will, necessarily, show a wide scatter in the obtained data.

Detailed descriptions of tests and of obtained test results were presented by Birmann [20], [21], Birmann and Raab [10], the Permanent Way Society of Japan [22], Bartlett [11], Prud'homme [23], I. A. Reiner [24] and others. A survey of results obtained by many investigators was presented in 1965 by J. W. Klaren and J. C. Loach [25] (Chapter 3) and more recently by P. Dogneton [26]. According to the conducted tests;

- (1) The resistance values depend upon the type of ties and ballast, as well as upon the tie spacing.
- (2) The resistance values increase with increasing weight of the rail-tie structure (they are also higher for the vertically loaded track).
- (3) The resistance values increase, up to a point, with increasing tonnage passed over the track (because of ballast compaction)
- (4) Track renovation work, which involves ballast disturbance (also by shovel packing or tamping), reduces the resistance values.
- (5) The resistance values depend on climatic factors, such as humidity and temperature. (e.g. frozen versus wet ballast and subgrade)

Results of tests, which demonstrate some of the above points, are shown in Figures 19 and 20.

For example, according to Birmann [20,21], depending on the track conditions, for a wooden tie track r_0 ranges from 400 kg/m (270 lb/ft) to 1800 kg/m (1200 lb/ft) and ρ_0 ranges from 400 kg/m (270 lb/ft) to 1500 kg/m (1000 lb/ft).

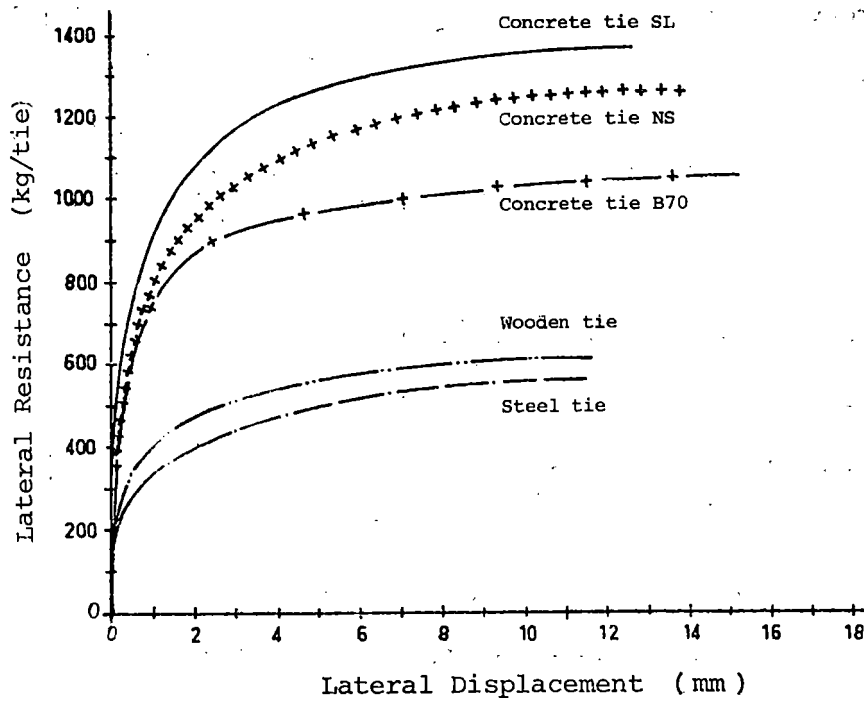
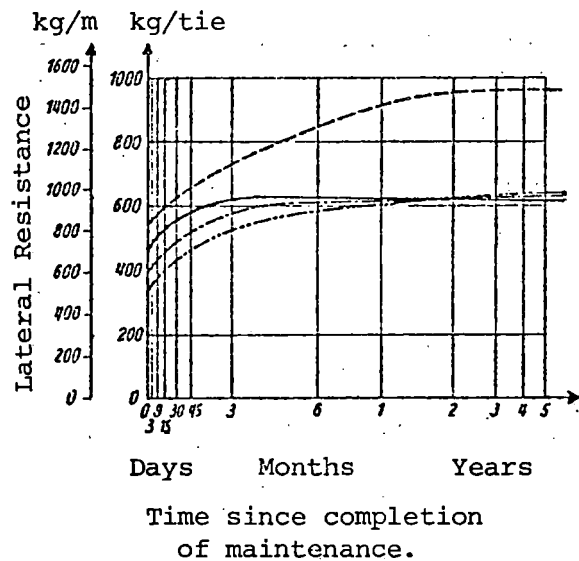


FIG. 19 DEPENDENCE OF LATERAL RESISTANCE ON TRACK STRUCTURE. NON-COMPACTED BALLAST [26].



(———concrete ties B62/B53;-----steel ties, K49;
 - - - - -soft wood ties, K49; - · - · - hard wood ties, K49)

Fig. 20 DEPENDENCE OF LATERAL RESISTANCE ON THE TONNAGE CARRIED OVER TRACK [10]

6. EXAMPLES

The purpose of this section is to show how the graphs presented in Section 4 can be used for analyzing thermal track buckling of tangent tracks.

Problem 1. *For an existing tangent track, determine the range of temperature increases above neutral which will not cause buckling.*

To analyze this problem first determine experimentally (or estimate) the anticipated resistance values ρ_0 and r_0 . For the present example assume that for an undisturbed track these values were found to be

$$r_0 = 1000 \text{ kg/m (672 lb/ft)}$$

$$\rho_0 = 1200 \text{ kg/m (800 lb/ft)}$$

Then, according to Fig. 18, for a track with 132 lb rails a safe temperature increase is $T_L = 48.50^\circ\text{C} = 87.5^\circ\text{F}$.

When utilizing the above result, it should be noted that $T_L = 48.50^\circ\text{C}$ is *not* the temperature increase at which the above track will usually buckle out, but rather the value which defines a range of safe temperature increases. In other words, as long as $T_0 < T_L$ the tangent track under consideration is safe against lateral buckling. The temperature increase which causes buckling is usually higher than T_L . As discussed in Section 4, it depends on geometric imperfections (and dynamic inputs); namely, the larger the imperfections the smaller the temperature increase which causes buckling. In this connection note that, according to the test results presented in Section 3, the temperature increases at which the equivalent test tracks buckled out were larger than 48.50°C .

When analyzing tracks, it should also be taken into consideration that, according to field observations, heated tracks have a tendency to buckle shortly after completion of track maintenance work, which involved ballast disturbance. The main reason for this is the resulting reduction of the ballast resistance values r_0 and ρ_0 , as described in Section 5. In order to determine the corresponding T_L temperature, the reduced values of r_0 and ρ_0 have to be used. Assuming that the experimentally determined values, for a freshly tamped track, are

$$r_0 = 500 \text{ kg/m}; \rho_0 = 600 \text{ kg/m}$$

then, according to Fig. 18, $T_L = 33.5^\circ\text{C}$ (60°F). Thus, a drop of 15°C (about a third of 48.5°C).

Next consider the case when the repair work is local, extending for example over only 15 meters (about 50 ft) of the track. It is reasonable to expect that if the heated track will buckle out laterally, it will do so in this region. For the corresponding analysis only the lateral resistance ρ_0 is reduced, since according to the made assumptions the main effect of the axial resistance r_0 is in the rather long adjoining regions, and they are not affected by the repair work. Assuming that for this case

$$r_0 = 1000 \text{ kg/m}; \rho_0 = 600 \text{ kg/m}$$

the graphs in Fig. 18 yield $T_L = 37^\circ\text{C}$. Thus, a drop of only 11.5°C .

The above numerical examples, in addition to showing how easily T_L may be determined by using Fig. 18, also demonstrate the effect of track maintenance work on the safe temperature increase.

Problem 2. For a tangent track, determine the installation (neutral) temperature in order to prevent track buckling by temperature increases and rail breaks by temperature drops.

The installation temperature of a jointless track depends on the temperature variations in the territory the rails are to be laid. A method for choosing the installation temperature is shown in Fig. 21. In this procedure, first determine from local records the highest and the lowest ambient temperatures which occurred in the particular territory during the past several decades. Then, introduce on a temperature scale the highest temperature expected in the rails (= highest recorded ambient temperature in region + temperature increase in rails above ambient) and the lowest temperature expected in the rails (= lowest recorded ambient temperature). Next, introduce on the temperature scale the T_L interval determined analytically (for the track under consideration) and then a T_f interval, as shown in Fig. 21(a). The overlap region of the T_L and T_f intervals is the range of safe installation temperatures.

The T_f value is the *safe temperature drop* which will not cause rail breaks during the low winter temperatures. This value depends on the metallurgy of the rails and of the welds, taking into consideration also their fatigue strength at low temperatures. For a method to determine the T_f value, used in the USSR, refer to [27].

As a numerical example, consider a territory where the highest and the lowest recorded ambient temperatures are $+110^{\circ}\text{F}$ and -30°F , respectively. Then, the highest temperature expected in the rails is $110^{\circ}+35^{\circ}=145^{\circ}\text{F}$, where 35°F is the assumed increase of rail temperature above ambient. The lowest temperature expected in the rails is -30°F . If for a 132 lb

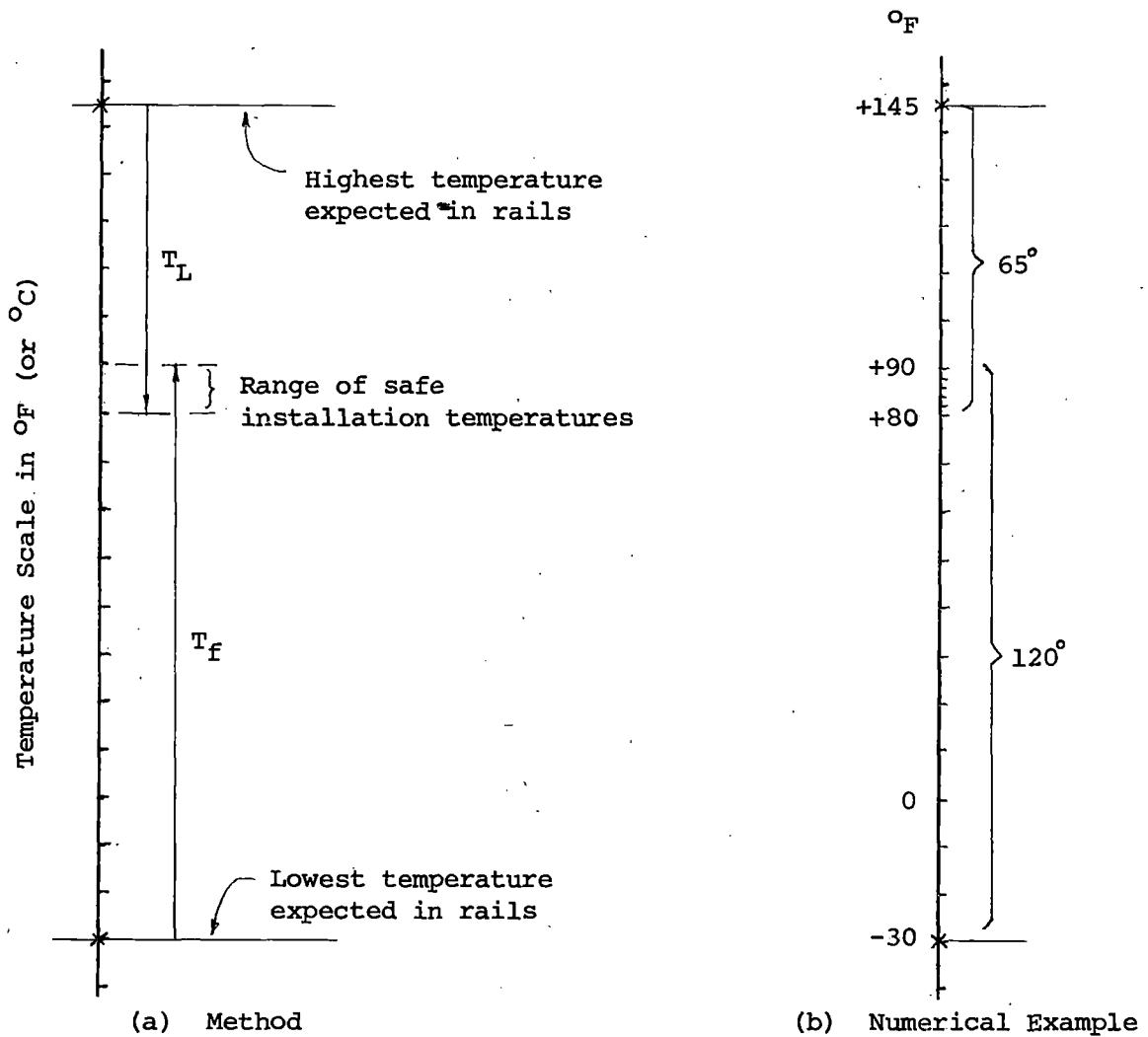


FIG. 21 METHOD FOR ESTABLISHING THE INSTALLATION (NEUTRAL) TEMPERATURE FOR A RAILROAD TRACK

track the analysis yields $T_L = 65^\circ\text{F}$ and the T_f value was found to be 120°F , then, according to Fig. 21(b), the rail installation temperature should be chosen from the range of 80° to 90°F .

When the T_L and T_f intervals do not overlap, the situation is more complicated. This may occur in the problem discussed above when, for example, the lowest recorded temperature is -50°F and $T_f = 90^\circ\text{F}$, as shown in Fig. 22(a).

One way to proceed in this situation, especially in signal territory, is to install the rails at 80°F in order to prevent the occurrence of track buckling, relying on the signalling system to detect rail breaks.

Another approach, utilized in the USSR [27], is shown in Fig. 22(b). This system requires two temperature adjustments per year; one in the spring and the other in the fall. Note that in Fig. 22(b) it was assumed that a range of installation temperatures is 10°F . Therefore, the shown temperature scheme is safe if after the spring adjustment the rail temperature does not drop below 0°F , and after the fall adjustment the rail does not exceed 95°F .

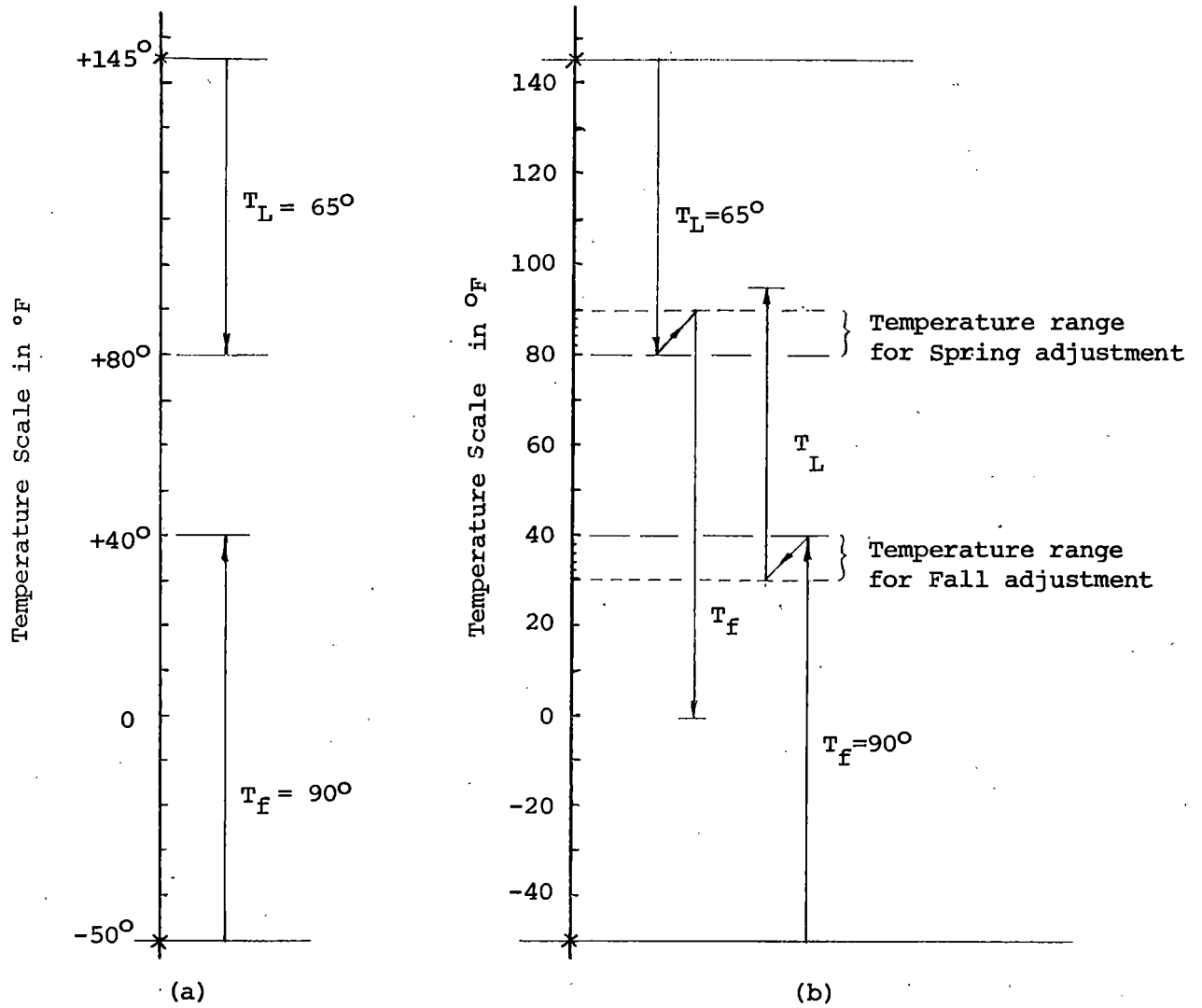


FIG. 22 DETERMINATION OF RAIL INSTALLATION TEMPERATURES FOR EXTREME TEMPERATURE CONDITIONS

7. MEASURES FOR PREVENTING THERMAL BUCKLING OF TANGENT TRACKS

From the discussion presented in the previous sections it may be concluded that in order to reduce the possibility of track buckling

(I) the track compression force should be as small as possible (without causing rail breaks during the winter), and

(II) the rigidity of the track structure (which consists of the rail-tie structure and the ballast) should be as high as possible.

Aim (I) may be achieved by installing and maintaining the rails at a neutral temperature, as determined previously in Problem 2. This method for determining the temperature, utilized by the railroads of the USSR [27], appears to be more appropriate than the method used by various European railroads which stipulate "that the rails should be free from stress within temperature limits near the *mean* of the extremes experienced" ([25] p.17 and Fig. 1).

Another measure for achieving aim (I) is to reduce the high rail temperatures by painting the rails white. According to Klaren and Loach ([25] p.60) tests were conducted in Holland in which the temperatures of whitewashed and regular rails in service were compared. It was found that on a hot sunny day the temperatures of the whitewashed rails were 5° to 7° C (9° to 12.5° F) lower than those of the unpainted rails. Although, presently, the painting of rails does not appear to be practical, this approach may be useful in special situations.

Aim (II) may be achieved by increasing the rigidity of the rail-tie structure and by increasing the ballast resistances r_o and ρ_o . To increase the rigidity of the rail-tie structure, many railroads abroad are using stiffer fasteners, such as the K-type and the spring clip fasteners. To achieve a high r_o value, the crib between the ties

have to be filled with well compacted ballast. Also heavier (concrete) and deeper ties increase the axial track resistance r_0 . Higher ρ_0 values may be achieved by increasing the ballast shoulder width, by raising the ballast shoulder, by increasing tie weight and cross sectional area, by using safety caps (which increase the tie area laterally) as shown in Fig. 23, and by compacting the ballast. Test results which demonstrate the effect of these measures on ρ_0 were presented by Dogneton [26].

To prevent track buckling, many railroads abroad found it necessary to increase the width of the ballast shoulder. For example, for tangent tracks, the DB and the railroads of the USSR increased the width to 35cm (14 inches). The standard practice on US railroads is to use a shoulder width of 6 inches [28]. Presently, it appears that the most economical and simplest way to reduce the occurrence of track buckling on US track is to increase the shoulder width, say to 15 inches on tangent tracks. It is reasonable to expect that this increased shoulder width will also reduce track degradation, and thus maintenance.¹⁾

Track maintenance practices should be such as not to violate the aims listed in (I) and (II). For example, they should not affect the effective neutral temperature of the rails, nor should they lower the ballast resistances excessively, during or before periods of large temperature increases. In this connection note that some railroads (for example, the SNCF) do not schedule track renovation work during the summer months whereas others (for example, the DB) allow it only for small specified temperature increases above neutral. It appears that renovation of a track is admissible when the highest expected rail temperature increase, above neutral, is lower than T_L .

¹⁾ The optimal width of the ballast shoulder, for preventing track buckling and reducing track maintenance, should be determined from tests.

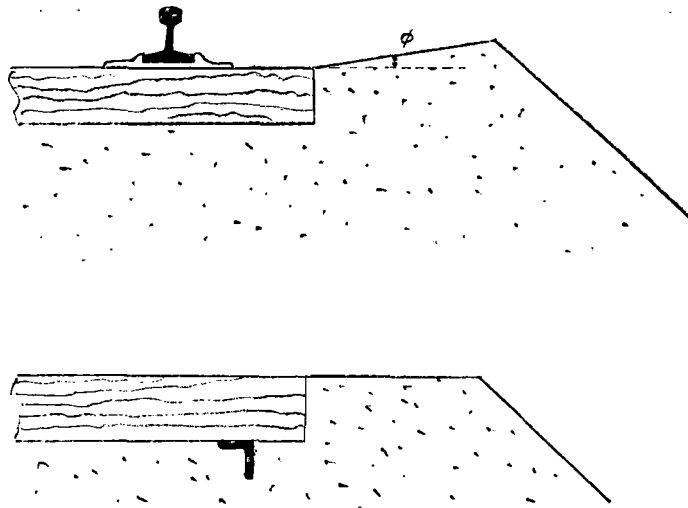


FIG. 23 MEASURES FOR INCREASING LATERAL RESISTANCE

REFERENCES

- [1] Haarmann, A., "Das Eisenbahn-Geleise" (The Railroad Track, In German), Vol. II, Kritischer Tiel, W. Engelmann, Leipzig, 1902, p. 262-263.
- [2] Wöhrl, A. "Experimentelle Grundlagen der Thermit-Schienenschweißung auf freier Strecke" (Experimental foundation of Thermit rail welding in a track, In German), Organ für die Fortschritte des Eisenbahnwesens, H.2, 1927, p. 23.
- [3] Rose, C. F., "Railway Accidents", Her Majesty's Stationary Office, London, 1970.
- [4] Albrekht, V. G., Bromberg, E. M., Ivanov, K. E., Liashchenko, V. N. Pershin, S. P., and Shulga, V. Ya., "Besstykovoi Put i Dlinnye Relsy" (The jointless track and long rails, In Russian), Izd. Transport, Moscow, 1967.
- [5] Kerr, A. D. "Lateral buckling of railroad tracks due to constrained thermal expansions - A critical survey", in Railroad Track Mechanics and Technology, Proceedings of a Symposium, held in 1975, A. D. Kerr Editor, Pergamon Press. (In print)
- [6] Kerr, A. D., "An analysis of thermal track buckling in the lateral plane", Federal Railroad Administration, DOT Report No. FRA-OR&D-76-285, 1976. Accepted for publication in Acta Mechanica.
- [7] Ammann, O. and Gruenewaldt, C. v., "Versuche über die Wirkung von Längs Kräften im Gleis" (Tests of the effect of axial forces in the track, In German), Organ für die Fortschritte des Eisenbahnwesens, Heft 6, 1932.
- [8] Nencsek, J., "Versuche der königlich ungarischen Staatsbahnen über die Standsicherheit des Gleises" (Tests of the royal Hungarian national railroads on track stability, In German), Organ für die Fortschritte des Eisenbahnwesens, Heft 6, 1933.
- [9] Kerr, A. D., "Model study of vertical track buckling", High Speed Ground Transportation Journal, Vol. 7, 1973.
- [10] Birmann, F., and Raab, F., "Zur Entwicklung durchgehend verschweißter Gleise. -- Ergebnisse bei Versuchen auf dem Karlsruher Prüfstand; Ihre Auswertung und Deutung" (To the development of the continuously welded track. -- Track results of the Karlsruhe test facility; their analysis and interpretation, In German), Eisenbahntechnische Rundschau, August, 1960.
- [11] Bartlett, D. L., "The stability of long welded rails", Parts I-IV, Civil Engineering and Public Works Review, 1960. Also "Die Stabilität durchgehend verschweißter Gleise," (The stability of continuously welded rails, In German), Eisenbahntechnische Rundschau, H. 1/2, 1961.

- [12] Bromberg, E. M., "Ustoichivost Besstykogo Puti" (The Stability of the jointless track, In Russian), Izd. Transport, Moscow, 1966.
- [13] Nemesdy, E., "Berechnung waagerechter Gleisverwerfungen nach den neuen ungarischen Versuchen" (Analysis of horizontal track buckling in accordance with the new Hungarian tests, In German), Eisenbahntechnische Rundschau, H. 12, 1960.
- [14] Numata, M. "Buckling strength of continuous welded rail" Bulletin International Railway Congress Association, English Edition, January 1960.
- [15] Prud'homme, A., and Janin, G., "The stability of tracks laid with long welded rails", Part I and II, Bulletin International Railway Congress Association, English Edition, 1969.
- [16] Kerr, A. D. "On thermal buckling of straight railroad tracks and the effect of track length on the track response", Princeton University Department of Civil Engineering Research Report 76-TR-19, 1976.
- [17] Kerr, A. D. "The effect of lateral resistance on track buckling analyses", Rail International, No. 1, 1976.
- [18] Kerr, A. D. "On the derivation of well posed boundary value problems in structural mechanics" International Journal of Solids and Structures, Vol. 12, Nr. 1, 1976.
- [19] Kerr, A. D. "On the stress analysis of rails and ties" Proceedings American Railway Engineering Association, Vol. 78, October 1976.
- [20] Birmann, F. "Das lückenlose Gleis" (The jointless track, In German), Die Bundesbahn, Heft 19, 1954.
- [21] Birmann, F. "Neuere Messungen an Gleisen mit verschiedenen Unterschwellungen" (New measurements on tracks with different ties, ballast and subgrade, (In German), Eisenbahntechnische Rundschau, Heft 7, 1957.
- [22] "The test on buckling of curved track" Permanent Way Society of Japan, Nr. 1, 1958.
- [23] Prud'homme, A. "The resistance of the permanent way to the transversal stresses exerted by the rolling stock" Bulletin International Railway Congress Association (English Edition), November 1967.
- [24] Reiner, I. A. "Lateral load test of track at Sabot, Virginia", U. S. Federal Railroad Administration, Report No. DOT-FRA-20015-S, 1976.
- [25] Klaren, J. W. and Loach, J. C. "Lateral stability of rails, especially of long welded rails", ORE Question D14, Interim Report No. 1, 1965.
- [26] Dogneton, P. "The experimental determination of the axial and lateral track-ballast resistance", Railroad Track Mechanics and Technology, Proceedings of a Symposium, A. D. Kerr Editor, Pergamon Press, (In print).

- [27] Basilov, V. V. and Chernisheva, M. A. "Spravochnik Inzhenera-Puteitsa" (Handbook of the track engineer. In Russian), Izdatelstvo Transport, Moscow, 1972, p. 654.
- [28] AREA Manual for Railway Engineering (Fixed Properties) Chapter 1, Roadway and Ballast, p. 1-2-7, 1975.

APPENDIX A: RAIL PROPERTIES

Rail type	Weight kg/m (lb/yd)	Area cm ² (in ²)	Moment of inertia with respect to centroid axis		Distance of centroid from base cm (in)	Height of rail cm (in)
			horizontal cm ⁴ (in ⁴)	vertical cm ⁴ (in ⁴)		
100 RE	50.35 (101.5)	64.19 (9.95)	2040 (49.0)		6.98 (2.75)	15.2 (5.98)
115 RE	56.89 (114.7)	72.58 (11.25)	2,731 (65.6)	450 (10.8)	7.57 (2.98)	15.2 (5.98)
119 RE	58.93 (118.8)	75.16 (11.65)	2,972 (71.4)	454 (10.9)	7.92 (3.12)	15.2 (5.98)
132 RE	65.53 (132.1)	83.55 (12.95)	3,671 (88.2)	607 (14.6)	8.12 (3.20)	17.8 (7.01)
136 RE	67.56 (136.2)	86.12 (13.35)	3,950 (94.9)	612 (14.7)	8.51 (3.35)	17.8 (7.01)
140 RE	69.75 (140.6)	89.03 (13.8)	4,029 (96.8)	616 (14.8)	8.56 (3.37)	17.8 (7.01)
P 50	51.51 (103.83)	65.8 (10.20)	2,037 (48.94)	377 (9.05)	7.09 (2.79)	15.2 (5.98)
P 65	64.93 (130.89)	82.8 (12.83)	3,573 (85.84)	572 (13.74)	8.17 (3.22)	18.0 (7.09)
P 75	75.1 (151.39)	95.8 (14.85)	4,597 (110.44)	771 (18.52)	8.41 (3.31)	19.2 (7.56)
S 49	49.43 (99.65)	62.97 (9.76)	1,819 (43.70)	320 (7.69)	7.29 (2.87)	14.9 (5.87)
S 54	54.54 (109.95)	69.48 (10.77)	2,073 (49.80)	359 (8.63)	7.50 (2.95)	15.4 (6.06)
S 64	64.70 (130.42)	82.70 (12.82)	3,252 (78.13)	604 (14.51)	8.06 (3.17)	17.2 (6.77)
UIC 54	54.40 (109.66)	69.34 (10.74)	2,346 (56.36)	418 (10.04)	7.49 (2.95)	15.9 (6.26)
UIC 60	60.34 (121.64)	76.86 (11.91)	3,055 (73.40)	513 (12.32)	8.09 (3.19)	17.2 (6.77)

(The P50, P65, and P75 data are those of 1961)

APPENDIX B :
REPORT OF INVENTIONS

The work involved the presentation of an improved analysis for predicting the safe temperature increase in the continuously welded rails of a railroad track, in order to prevent thermal track buckling, and a discussion of preventive measures. After a review of the work performed under this phase of the contract, it was determined that no discovery, or invention has been made, however the work did result in a better understanding of the determination of safe installation temperatures for continuously welded rail.

Thermal Buckling of Straight Tracks
Fundamentals, Analysis and Preventive
Measure (Interim Report), 1978

**Thermal Buckling of Straight Tracks
Fundamentals, Analysis and Preventive
Measure (Interim Report), 1978**
US DOT, FRA

U.S. DEPARTMENT OF TRANSPORTATION
FEDERAL RAILROAD ADMINISTRATION
Washington, D.C. 20590

Official Business

PENALTY FOR PRIVATE USE, \$300

PROPERTY OF FRA
RESEARCH & DEVELOPMENT
LIBRARY

POSTAGE AND FEES PAID
FEDERAL RAILROAD
ADMINISTRATION

DOT 516

